Radiological and Nuclear Countermeasures Program

Securing America against unconventional attacks

FEBRUARY 2009

LLNL-TR-411374

The Effect of Gamma-Ray Detector Energy Resolution on the Ability to Identify Radioactive Sources

Lawrence Livermore National Laboratory

Karl E. Nelson*

Thomas B. Gosnell

David A. Knapp

*925-424-4183 • nelson85@llnl.gov

Lawrence Livermore National Laboratory

The Effect of Gamma-ray Detector Energy Resolution on the Ability to Identify Radioactive Sources

February 2009

*Karl E. Nelson**

Thomas B. Gosnell

David A. Knapp

LLNL-TR-411374

*925-424-4183, nelson85@llnl.gov

Lawrence Livermore National Laboratory
P.O. Box 808 · Livermore, CA 94551-0808

[This page intentionally left blank.]

Executive summary

This report describes the results of an initial study on radiation detector spectral resolution, along with the underlying methodology used. The study was done as part of an ongoing effort in Detection Modeling and Operational Analysis (DMOA) for the DNDO System Architecture Directorate. The study objective was to assess the impact of energy resolution on radionuclide identification capability, measured by the ability to reliably discriminate between spectra associated with "threats" (defined as fissile materials) and radioactive "non-threats" that might be present in the normal stream of commerce. Although numerous factors must be considered in deciding which detector technology is appropriate for a specific application, spectral resolution is a critical one for homeland security applications in which a broad range of non-threat sources are present and very low false-alarm rates are required. In this study, we have proposed a metric for quantifying discrimination capability, and have shown how this metric depends on resolution. In future work we will consider other important factors, such as efficiency and volume, and the relative frequency of spectra known to be discrimination challenges in practical applications.

Study Approach

To capture the range of gamma-ray sources and shielding configurations found in commerce, we generated simulated populations of 1000 or more spectra, each with 3000 energy channels. We then analyzed this spectral data set using a well-known technique of multivariate statistical analysis, *Principal Component Analysis* (PCA). Although much of our effort focused on discrimination within a complex population of deterministic spectra, rather than statistical samples from a population, we found the PCA framework useful in quantifying our analysis. In particular, we defined a metric to measure information content of gamma-ray spectra (as a function of detector resolution) as the number of *principal components* required to approximate an observed spectrum to a specified accuracy. We explored the behavior of this information-content metric as a function of detector resolution.

We also developed a library of spectral templates to span the set of spectra expected to be encountered in realistic applications and then simulated idealized detector responses with different energy resolutions. The information-content metric was calculated and used to determine the point at which additional resolution provides only marginal additional discrimination capability over the entire set of spectra. We then demonstrated detector performance at different resolutions using a simplified identification problem (discriminating "threats" from "non-threats") to estimate a limit on performance for a given resolution.

In this study, we examined a range of energy resolutions from 0.25% (highest resolution) to 8% (lowest resolution). This wide range of resolutions was investigated to determine whether intermediate resolutions might be useful alternatives to those of germanium (Ge) (0.25% and above) and sodium iodide (NaI) (7–8%), two of the most common detector types currently in use for source identification.

Key Findings

We have developed an information-content metric that allows direct comparison of the ability of detection systems to correctly distinguish between threat and non-threat sources. In this initial study, we demonstrated that, at moderate count rates, unambiguous discrimination of potential

threat sources from non-threat sources in the presence of background requires a detector energy resolution of at least 1%. We say at least 1% because our analysis is based on simulations that have not captured all of the physical effects that occur in real-world systems.

At present, only semiconductor detectors have an energy resolution better than 1%, and within this class, only Ge has been demonstrated as a practical detector material. Unfortunately, Ge has major drawbacks that have limited its widespread adoption for threat detection: it is costly in comparison to NaI; it does not come in the large sizes needed for some applications such as portal monitoring (requiring their use in arrays); and it requires cryogenic cooling. Our analysis indicates that there is value in developing detectors with improved energy resolution relative to fielded NaI systems that avoid the complications of Ge detectors. For effective performance in threat detection and classification applications, such detectors do not need the resolution of Ge.

From a technology development perspective, this means that mass producing and "ruggedizing" laboratory-quality Ge detectors (to preserve the resolution capability) may not be the only viable path. This is not a new concept; materials such as HgI and CZT have been studied for many years, but have only found niche applications if at all. Ongoing research may lead to detectors with properties more desirable for critical homeland security applications.

Study Limitations and Future Research

The topic of this initial study, detector resolution, is only one attribute that must be considered in selecting a detector for a given application. Other factors that do not impact discrimination capability (e.g., cost, size, weight, ruggedness, reliability, comfort, covertness, power consumption, operating temperature and humidity ranges, and user interface) are all important. We do not offer a simple rule for making such a complex decision. We do, however, provide a quantitative framework for assessing the discrimination performance of a given resolution in various applications, viewed in terms of detector counts available for discrimination algorithms. Detector counts available in practice will be highly application-specific and will depend on other detector properties such as efficiency and volume. Future work should include evaluation of the impact of these properties on the same information metric used for the current resolution study.

The study is a bounding analysis and as such omitted many factors that complicate detector performance in realistic applications, such as calibration errors and background interference. Including such factors in our analysis would result in worse detector performance, although we have not quantified how much worse it might be. In addition, we have used simplified, one-dimensional deterministic radiation transport models for this study. More detailed, three-dimensional Monte Carlo models should be used to verify results and to explore additional aspects of detector design.

Detector deployment is also influenced by the nature of operationally relevant factors. For example, for routine screening of objects (vehicles, people, etc) at choke points—such as portals or approaches to bridges or tunnels—factors such as traffic volume, capacity for secondary inspection, and frequency of the most challenging benign nuisance sources will all be important in determining detector performance. Case studies of operational environments can elucidate the complex interactions among multiple detector properties and environmental parameters.

Contents

Acknowledgements

The authors would like to thank Stanley Prussin, Dan Dietrich, Wolfgang Stoeffl and Simon Labov of Lawrence Livermore National Laboratory for their valuable comments and suggestions during this study. In addition, we acknowledge the important role served by the software package GADRAS, developed by Dean Mitchell of Sandia National Laboratories. This work was supported by the Systems Architecture Directorate within the Domestic Nuclear Defense Office.

1.0 Introduction

This report presents an initial systematic treatment of gamma-ray detector energy resolution, a critical property of radiation detectors that decision makers must consider as part of the effort to detect and interdict the illicit transport of radiological and nuclear weapons or the radioactive materials needed to make them.

Since September 11, 2001, there has been an increasing interest in the detection of nuclear threats in commerce, especially with large radiation detectors at fixed portals or with hand-held instruments. In this paper we concentrate on gamma-ray detectors and, in particular, on *one* of the most important features of these detectors—energy resolution and its effect on the ability to reliably identify radioactive sources or at least classify them as "threat" or "non-threat."

We have developed a quantitative view of energy resolution for gamma-ray detectors based on an examination of the information content available from different detector types. Our assessment had two distinct approaches. First, we developed a metric for measuring the information content of gamma-ray spectra as a function of energy resolution. This metric, based on principal components of variance (discussed later), provides insights as to what energy resolution is required to extract the bulk of available spectral information. The metric was also used to determine the number of counts required in a gamma-ray spectrum such that full information content can be extracted. Information estimates were performed with a simplified physics model, so our results can be viewed as bounding the amount of information that can be extracted. However, a bulk information metric can only determine how well one can separate radionuclides in general, but not in specific cases of interest. To address this problem, our second approach was to perform a bounding case study for unambiguous identification based on known problem cases from previous studies of radionuclide identification algorithms.

Before we delve into an advanced discussion of energy resolution, for readers not steeped in nuclear technology, we present a brief review of nuclear terminology, radioactivity in general, gamma radiation in particular, gamma-ray measurement instruments and methods, and a traditional view of gamma-ray detector resolution and its effect on the ability to identify unknown radioactive sources (detector sensitivity).[1] The reader already familiar with this material is invited to skip directly to Section 3.0, "Energy-resolution study: methodology and results," where the principal analysis and findings of our work are described.

2.0 Review of the fundamental principles of gamma-ray detection and energy resolution

2.1 About the atomic nucleus

All matter, of course, is composed of atoms. Atoms comprise a tiny nucleus with a positive electrical charge surrounded by a cloud of negatively charged electrons. The nucleus contains two types of particles of almost identical mass—neutrons and protons. Neutrons have no

[1] To keep the current report self-contained, we have drawn liberally from [K1] for our discussion in Section 2 and several of the appendices. This source provides an excellent detailed treatment of the basic principles of radiation detection.

electrical charge and protons have a positive electrical charge equal to but opposite of the electron's charge. The number of protons in the nucleus (variously called its atomic number or element number and indicated by Z) determines the atom's chemical element. For example, all hydrogen atoms have one proton, all iron atoms have 26 protons, and all uranium atoms have 92 protons. The nuclei of all of the chemical elements can vary in their number of neutrons. These variations among an individual element are called *isotopes*. Generically, all nuclear species, regardless of element, are referred to as *nuclides*. The symbol we use to denote a particular nuclide is a superscript that indicates the nuclide's total number of protons and neutrons, A, followed by its chemical symbol that implicitly indicates Z. For example ^{60}Co has a total of 60 neutrons and protons, and has 27 protons, as do all isotopes of cobalt.

2.2 Radioactivity

For the atomic nucleus to remain stable, it must have a proper balance of neutrons and protons. A nucleus with too many or too few neutrons is unstable, much like a stretched spring. It is called a parent nucleus and seeks stability by emitting nuclear particles, by capturing an orbital electron, or even by heavy nuclei splitting in two (*nuclear fission*) to produce two smaller nuclei. The residual nuclei in all of these processes are called daughter nuclei and differ from the parent by a change in Z, A, or both. These are the processes of radioactive decay. Isotopes or nuclides that are radioactive are called *radioisotopes* or *radionuclides*.

A variety of subatomic particles and electromagnetic radiations can be emitted during radioactive decay. Collectively, they are all aspects of *radioactivity*. Because of their ability to escape from items surrounded by thick materials and still be observed by external radiation detectors, two of these emissions are relevant to detection at a distance: neutrons and gamma rays.

2.3 About gamma rays

Following initial radioactive decay, the daughter nucleus, will, in almost all cases, not yet have achieved stability but will have reached a discrete excited state of the daughter. In the overwhelming majority of cases, the lifetime of this state is exceedingly brief (less than 10^{-8} to 10^{-10} seconds) and is culminated by the emission of a quantum of electromagnetic radiation, a gamma ray, with a discrete energy that is unique to the daughter nucleus.[2] Depending on the particular nuclide undergoing radioactive decay, the emission of a single gamma ray may not complete the de-excitation of the daughter but may reach another intermediate excited state from which yet another gamma ray of unique energy is emitted. It is not uncommon for cascades of several gamma rays to be emitted before reaching the ground state of the daughter nucleus.[3] Furthermore, the daughter nucleus may itself be radioactive, leading to further radioactive decay. For example, the naturally occurring radionuclide ^{238}U decays through 13 generations of radioactive daughters before finally reaching the stable nuclide ^{206}Pb.

---

[2] Internal conversion is a process that competes with gamma-ray emission. In this case, the nuclear excitation energy is transferred directly to one of the orbital electrons of the atom that is then ejected with energy equal to the nuclear excitation energy minus the binding energy of the electron.

[3] The daughter nucleus may have a number of excited states that can be reached with varying probability by the initial decay. The gamma ray(s) emitted from each excited state are unique. This results in a complex pattern of gamma-ray emission over time as a large number of these same nuclides decay to different excited states.

The energy range of the vast majority of gamma rays from nuclear decay is roughly 10 to 3000 keV.[4] Some gamma rays of potential interest of up to 12,000 keV occur as the result of nuclear reactions.

Because the gamma rays emitted during decay of a specific radionuclide are *discrete and unique,* they provide a *nuclear fingerprint* that can potentially be exploited to identify the parent radionuclide.[5] Identifying a radionuclide from its characteristic energy pattern (*spectrum*) of gamma rays becomes more difficult when they are transported through intervening material before reaching the detector. Such material can completely absorb low-energy gamma rays or can cause partial energy loss (*Compton scattering*) in others, resulting in a distortion in the pattern that is a function of gamma-ray energy, material type, and thickness. This problem is discussed further in Appendix D (Section D-3, "The effect of shielding on source identification").

2.4 Gamma-ray detection

In order to exploit a radioactive source's gamma-ray fingerprint, we require a radiation-monitoring instrument that is able, as closely as possible, to extract the energy pattern of gamma rays incident upon it, a *gamma-ray spectrometer*. This begins with an energy-resolving detector assembly that ultimately produces charge carriers whose number is proportional (or nearly so) to the amount of gamma-ray energy deposited in the detector. As each gamma ray interacts with the detector the charge carriers are electronically processed and converted into a voltage pulse with a height that is proportional to the number of charge carriers and thus the energy deposition as well. The pulse height is then digitized and one count is added to a computer-type memory register, called a *channel*, that corresponds to a narrow energy range that is appropriate for that gamma ray. There are many contiguous memory channels that together span the energy range of interest for the measurement. As gamma ray data acquisition continues, each additional individual gamma ray adds a count to the channel that is appropriate for its amount of energy deposition.

After a sufficient number of counts are acquired, the memory can be read out and the results plotted as a series of dots representing the number of counts vs. pulse height. Frequently the pulse-height axis is calibrated to represent gamma-ray energy deposition (see **Figure 1**). This plot is properly called a gamma-ray pulse-height distribution, although nuclear scientists by convention, if not entirely accurately, call it a gamma-ray spectrum. In the rest of this paper, we will follow the latter convention.

---

[4] Kiloelectronvolt, keV, an energy unit appropriate for gamma rays equal to 1.602×10^{-16} joules.

[5] While the discrete gamma-ray energy is unique to the daughter nucleus, in some circumstances some of the same excited states of a daughter nucleus can be populated by the decay of different parents. An example is the pair of medical radionuclides ^{67}Ga and ^{67}Cu that both populate some of the same excited states of the daughter nuclide ^{67}Zn. The fraction of decays that populate the daughter states differs for each parent nuclide so that the parent can be identified from the relative emission rates of the daughter gamma rays.

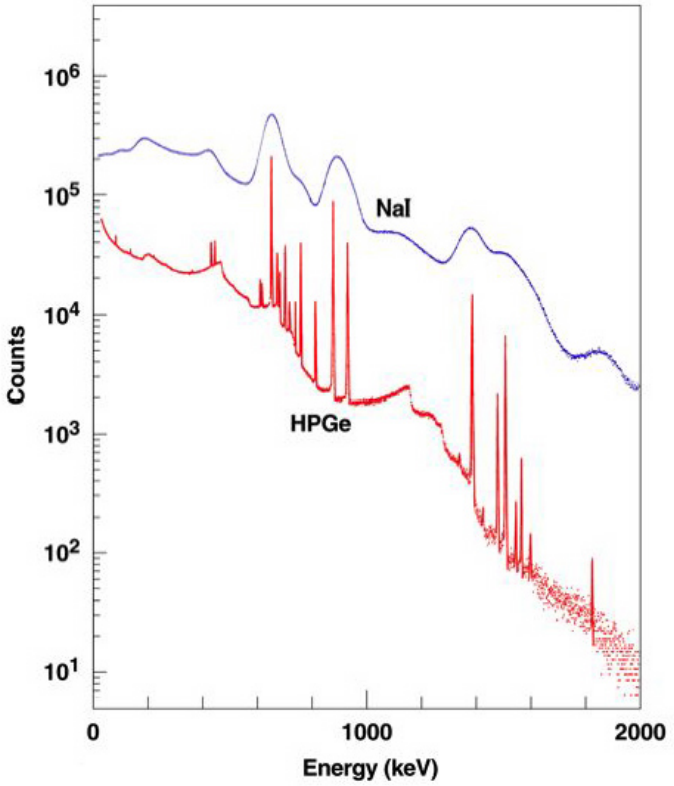

Figure 1. Gamma-ray spectra of a modestly complex mixture of silver isotopes ^{110m}Ag and ^{118m}Ag taken with NaI and Ge [(Ge(Li)] detectors.[6] ^{110m}Ag is an industrial calibration and gauging source and ^{108m}Ag is a byproduct of ^{110m}Ag production. There is a considerable mixing of gamma rays from each isotope in the spectra that is resolvable in the Ge spectrum but not in the NaI spectrum. Figure adapted from [P1].

When gamma rays of a particular characteristic energy (often called lines) deposit their full energy in a detector, a peak will appear in the gamma-ray spectrum—*a full-energy peak* or *photopeak*—that indicates full energy deposition. Gamma rays do not always deposit their full energy in the detector. They often scatter, causing partial energy deposition, and the scattered gamma ray escapes from the detector. Pulses from partial energy deposition are found in a continuum (the *Compton continuum*) in the spectrum below the full-energy peak. When some unusual radionuclides decay they will always decay directly to the ground state of the daughter with no gamma-ray emission.[7] Usually radioactive decay produces one to several to many characteristic gamma rays of differing energies and varying intensities. The full-energy peaks

[6] Early germanium detectors made with normal semiconductor purity could not attain the large depletion depth (active detection volume) needed for gamma-ray measurements. This was resolved by adding a tiny amount of Li dopant to the Ge to compensate for the impurities. The resultant crystals were designated Ge(Li). Subsequently, the ability to grow extremely pure Ge was developed and Ge detectors of all sizes are now produced with this material without having to resort to Li doping. These newer detectors are called high-purity germanium and designated HPGe. The important performance characteristics of both of these types of detectors are that their energy resolution and efficiency are essentially identical.

[7] Almost all radionuclides that can be encountered in commerce emit characteristic gamma rays. An important exception is ^{90}Sr that decays by beta particle emission to the ground state of its radioactive daughter ^{90}Y. ^{90}Y almost always decays to the ground state of its stable daughter ^{90}Zr ,but does emit two known high-energy gamma rays with extremely low emission probabilities on the order of 10^{-6}% [B1].

that they produce in the gamma-ray spectrum, if they can be fully resolved from other structure in the spectrum, provide the unique and most robust aspects of their gamma-ray fingerprint.

2.5 Detector properties essential for radionuclide identification

The ability of the detector in a gamma-ray spectrometer to be useful for identifying unknown radioactive sources depends critically on three factors: energy resolution, detection efficiency, and, a property that is a function of the first two, detection sensitivity. While this paper focuses primarily on energy resolution, its importance cannot be adequately addressed unless presented within the context of detection efficiency and sensitivity; so all three are discussed in this paper.

2.5.1 Gamma-ray detector energy resolution

As noted above, when gamma rays interact with material, such as a detector, the material can completely absorb the gamma ray's energy in some cases or can cause partial energy deposition in others. Imagine measuring a radionuclide that emits gamma rays at only one energy. Ideally the detector would always absorb all of the gamma ray's energy and its energy deposition would be recorded exactly in a single memory channel, as at E_0 in **Figure 2**. However, for a gamma ray incident on the detector with energy in the range of roughly 300–3000 keV, its most common initial interaction is Compton scattering. In this case a portion of the gamma-ray energy is transferred to an electron and its energy is absorbed. The scattered gamma ray can go on to further interactions or escape from the detector causing a count to appear in the gamma-ray spectrum below the channel corresponding to full-energy deposition (this is illustrated in Figure 2 as "Theoretical"). Normally, all scattering angles can occur in the detector. Therefore a continuum of energies can be transferred to the electron, ranging from zero up to the maximum amount of possible energy transfer as indicated by the vertical edge pointed to by the left-hand "Theoretical" arrow in Figure 2.

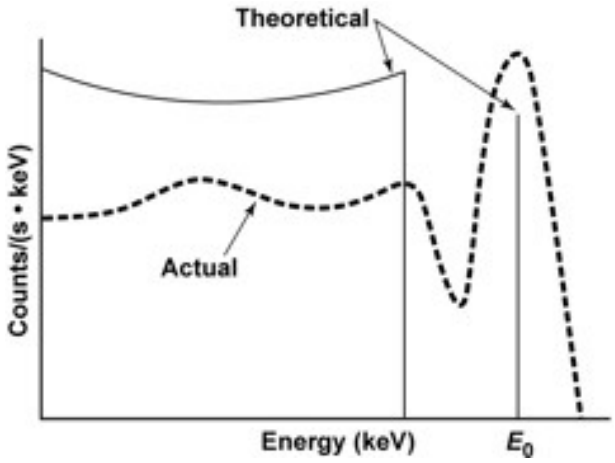

Figure 2. Theoretical gamma-ray spectrum from a nuclide emitting gamma rays at a single energy, E_0. A line of negligible width appears representing full energy deposition at E_0 with a Compton continuum extending from zero energy to its maximum. The dashed line labeled "Actual" is a schematic representation of the output of a gamma-ray measurement that indicates the broadening of the spectrum by the response function of the detector and the real-world effect of gamma rays—the broad peak at mid-continuum—that entered the detector after first undergoing Compton scattering in adjacent materials [H1].

The dashed line in Figure 2 indicates the response of a real detector. The width of the dashed full-energy-deposition peak about E_0 in Figure 2 is referred to as the energy resolution of the detector, R. It is commonly referenced to the full width at half the maximum height (FWHM) of a peak at 662 keV from the single-gamma-emitting nuclide, ^{137}Cs, as shown in **Figure 3**, where the pulse height H_0 corresponds to an energy deposition of E_0 (H_0 is proportional to E_0).

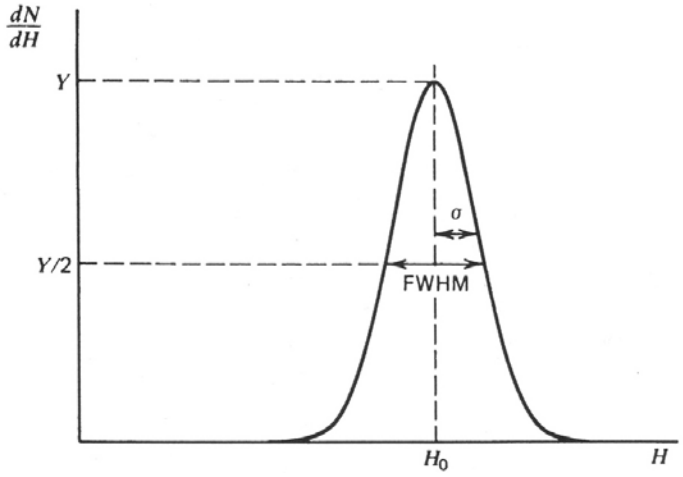

Figure 3. Definition of energy resolution, *R* (taken from [K1]).

Detector resolution is then defined as the ratio of the FWHM to H_0:

$$\text{Resolution } R = \frac{FWHM}{H_0} \tag{1}$$

Clearly the lower R is, the better the energy resolution and the better the detector's ability to resolve closely spaced peaks. **Table 1** displays the nominal energy resolution measured at 662 keV, density, and Fano factor (discussed later) for a number of gamma-ray detectors.

Table 1. Salient characteristics of frequently used gamma-ray sensors

Sensor material	Detector type	Energy resolution (%)	Density, ρ (g/cm^3)	Fano Factor
Polyvinyl Toluene—PVT	Scintillation	~25*	1.03	(≈1)
Sodium Iodide—NaI(Tl)	Scintillation	5–8	3.67	≈1
Cadmium Zinc Telluride—CZT	Semiconductor	1–10	5.78	<0.2
Lanthanum Bromide—$LaBr_3$	Scintillation	3	5.29	≈1
Germanium—Ge**	Semiconductor	0.25	5.32	0.08

* Because full-energy peaks are so insignificant in PVT as to be of negligible utility, the definition of energy resolution from Eq. 1 is not applicable.
** Must be cryogenically cooled when making gamma-ray measurements. A mechanically cooled handheld Ge detection system is commercially available [O1].

Of the detectors listed in Table 1, the most often used are NaI and Ge. For a visual example of their dramatically different response to gamma rays see Figure 1. Factors that contribute to energy resolution are discussed in Appendix A.

2.5.2 The value of good energy resolution for source identification

Many types of sources are encountered in commerce. Most are benign and some have complex gamma-ray spectra, which is typical of background radiation as well. Practical experience has shown that the key to having confidence that an unknown spectrum is not from a threat source is having confidence that it is from a benign source. Good energy resolution provides greater confidence in the identification of complex sources, both benign and threatening. *"Virtually all gamma-ray spectroscopy that involves complex energy spectra is now carried out with germanium detectors"* [K3].

"Not only does good resolution help separate closely spaced peaks, but it also aids in the detection of weak sources of discrete energies when superimposed on a broad continuum. Detectors with equal efficiency will result in equal areas under the peak, but those with good energy resolution produce a narrow but tall peak that may then rise above the statistical noise of the continuum. This effect is illustrated in" ...[**Figure 4**]... *"in which the only variation between spectra is the resolution* [K5]*."*

Plutonium and HEU are weakly emitting gamma-ray sources and are relatively easy to mask or shield (especially HEU). In Appendix C, simple statistical considerations show that for weak peaks where the source emission rate is small relative to the continuum count rate, *the data acquisition time required to make a peak detection, t_m, increases nearly in direct proportion to the energy resolution, i.e. $t_m \propto R$. This is a significant disadvantage for low-resolution (high value of R) detectors.* Because good germanium systems will have a typical energy resolution of a few tenths of a percent compared with 5–10% for sodium iodide, we can see NaI resolution is typically a factor of 25–32 worse than that of germanium.

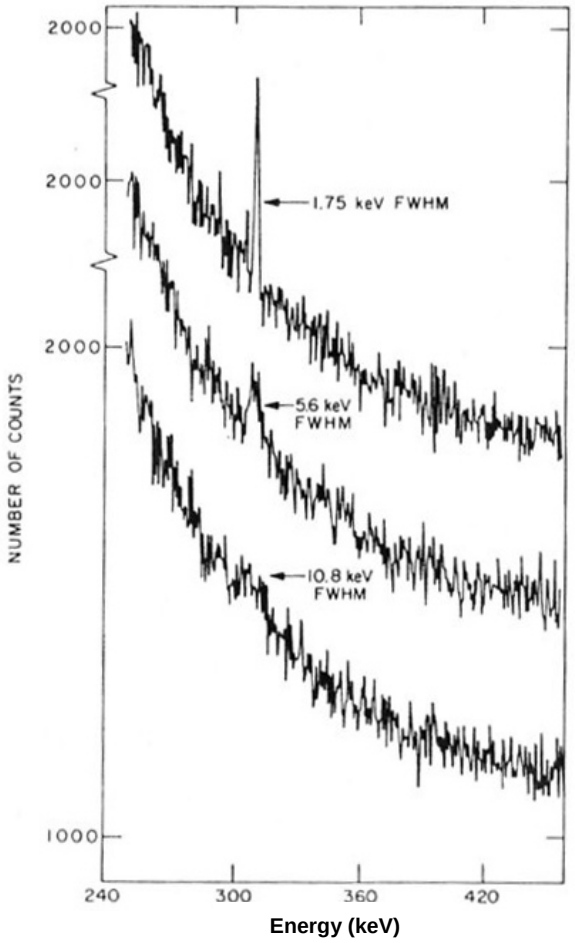

Figure 4. Effect of energy resolution degradation on peak detection sensitivity. The figure shows a portion of three gamma-ray spectra taken with a germanium detector. Increasing amounts of white noise were electronically introduced into the spectrum in order to study the effect on peak detection as a function of energy resolution. In the top spectrum in the figure, the absolute energy resolution is 1.75 keV and the peak is clean and manifest in the spectrum. When the resolution was degraded to 5.6 keV, the peak was ragged but still detectable. With further resolution degradation to 10.8 keV, the peak is essentially undetectable [A1].

This disadvantage is mitigated to some extent by analysis of the full NaI spectrum rather than individual photopeaks (Appendix D). Full spectrum analysis of NaI spectra can be automated with considerable improvement over attempts at photopeak analysis or energy-region-of-interest ratios. There remain, however, some ambiguous but potentially provocative NaI spectra that are now referred to specialized experts for analysis by rapid radiation transport modeling. The authors are confident that many of these spectral analyses could have been resolved without referral to this cadre of experts had the spectra been acquired and analyzed with Ge detection systems.

2.5.3 Detector efficiency

Detector efficiency is the probability that a detector will record a gamma ray that is incident upon it. Because much of this paper will focus on photopeaks, we are interested in the *intrinsic peak efficiency,* ε_{ip}, which is defined as:

$$\varepsilon_{ip} = \frac{\text{number of pulses recorded in photopeak}}{\text{number of radiation quanta incident on detector}} \quad (2)$$

The intrinsic peak efficiency depends primarily on the detector material, the incident gamma-ray energy, and the physical thickness of the detector in the direction of the incident radiation. For this reason, to cover the wide range of energies required for successful radionuclide identification in commerce, even hand-held detectors have thicknesses (depth) exceeding 25 mm. The general-purpose gamma-ray detectors used for source identification are formed as right circular cylinders with a diameter roughly equal to the depth. A deep pencil-thin detector would rarely record a full-energy peak as its surface area would be too small to intercept many gamma rays and most of those that it did intercept would scatter in the detector and exit through the side without depositing all of their energy.

The factors related to detector efficiency are discussed in more detail in Appendix B, including interaction of radiation with matter as a function of gamma-ray energy, effect of shielding on full-energy peak formation, and the importance of detector volume on detection efficiency.

2.5.4 Detector sensitivity

"The sensitivity of a gamma-ray spectrometer is a measure of its ability to detect a gamma-ray peak in the presence of interference from natural radioactivity and Compton scattering of higher energy gamma rays originating in the source [C1]*."*

Clearly, for a radiation detector, the degree of the response needs to be high enough to detect a useful signal. Moreover, it needs to be high enough to detect this signal within an operationally acceptable period of time in the presence of interferences from natural radioactivity and Compton scattering from higher energy gamma rays originating in the source. The sensitivity is of greatest importance when the interference is comparable to or greater than the source signal intensity. When monitoring for the presence of threat sources, sensitivity is of considerable importance when those sources are shielded and/or weakly radioactive, as in the case of uranium or plutonium. Detector sensitivity is expressed by its signal-to-noise ratio, ρ, for a given peak. An expression for ρ is derived in Appendix C along with an expression for the minimum data acquisition time, t_m, required to attain a desired value of ρ. *These expressions are functions of both the detector's energy resolution and detection efficiency.*

2.6 How good does energy resolution really need to be?

"The energy resolution of scintillators is poor. The comparative spectra shown in ...[Figure 1]*... illustrate the clear superiority of germanium detectors in situations where many closely spaced gamma-ray energies must be separated* [K5]*."*

Why, in spite of the difficulties associated with their use, do people continue to attempt source identification with NaI detectors? There are two principal reasons: (1) Ge detector systems are more expensive, although costs are declining and (2) Ge detectors need to be cryogenically cooled, an operational nuisance. The detector cited in [O1] has an integral mechanical cooler, but is still not as convenient as a detector that works at ambient temperature.

It has long been known to experts in spectroscopy that a minimum required resolution, a critical point, is needed for high-confidence source identification, especially by automatic computer

analysis. From the discussion of spectrum analysis above, detectors that have adequate energy resolution to provide well-defined, isolated full-energy peaks are easier to analyze and less likely to lead to ambiguous results. Largely for this reason, most experts in gamma-ray spectrometry generally place this critical point of minimum required energy resolution somewhere significantly better than NaI resolution.[8] This view was developed largely on the basis of attempting to analyze either NaI data or Ge data. There are few detectors with resolutions between these two in the field. The only other deployed detector materials with resolution between NaI and Ge are CZT semiconductor crystals, which are too thin to effectively absorb gamma rays of all but the lowest energies, and $LaBr_3$ scintillators. Prior to the current study, it has been unclear as to where the critical point of sufficient energy resolution occurs.

The simple models that we have introduced in this section and supplementary appendices do not give any guidance as to what resolution is required to identify sources or how one should trade off efficiency with energy resolution. A more sophisticated and quantitative model-based approach to determining the critical range of energy resolutions is essential for guiding efforts to develop new detector materials or to significantly improve detectors based on existing materials. Such an approach is discussed next.

3.0 Energy resolution study: methodology and results

In our effort to address the general problem of required energy resolution, we performed a theoretical study designed to quantitatively determine the impact of detector energy resolution on the ability to unambiguously identify radioactive sources or to distinguish threat sources from non-threat sources.

The study consisted of four phases: first, we designed a methodology for quantitative estimation of the information content of a gamma spectrum, and used it to characterize the information content of arbitrary noise-free spectra. Next, we investigated the information content of synthetic noise-free spectra that would be emitted by real-world radioactive sources in a variety of shielding configurations. Third, we investigated the impact of statistical noise on the information content of the simulated spectra and its interaction with the detector energy resolution. Finally, we estimated real-world performance in distinguishing threat from non-threat sources for realistic simulated spectra.

To eliminate variables of detector size, efficiency and stopping power, all the results were normalized to a 140% Ge detector. In other words, these results simulate the performance of this detector with everything held constant except the resolution. Because the energy resolution of real-world detectors is not a constant fraction of the energy, the resolution was defined as the fractional resolution at an energy of 662 keV (the energy of the primary ^{137}Cs gamma-ray line) and the variation with energy was simulated using the detector response function calculated by the GADRAS program [M1].

[8] This has inspired continuing efforts over decades to develop semiconductor detectors that have energy resolution considerably superior to NaI, yet can operate at ambient temperature.

3.1 Estimation of information content in gamma-ray spectra

For threat/non-threat discrimination, a detector is called upon to differentiate between more than 100 radiation sources, each with a variety of shielding configurations. A few of these are threat sources, but the vast majority are benign sources commonly encountered in commerce that must not be falsely identified as threat sources. The gamma-ray spectra for this large group of sources range from the simple to the bewilderingly complex.

For this study, we created our populations of gamma-ray spectra using computer simulation. Each of these spectra contains 3000 energy channels. We view a spectrum as a vector with 3000 independent variables. Any vector can be thought of as a single point in a space with as many dimensions as there are variables. The distance of the point from the origin of the multidimensional coordinate system is a measure of the magnitude of the vector or, in our case, the strength of the gamma-ray signal represented by the vector. The gamma-ray spectrum populations that we will examine typically represent hundreds of data points in a space of 3000 dimensions.

In light of the complexity of the problem we are attempting to solve, we cannot address it with a simple model. There are simply too many different radionuclides and shielding configurations to attempt to address each individually. Because changes in any single parameter, including shielding or source material, will cause changes in many energy channels throughout the observed spectrum, the problem has characteristics similar to those encountered in high-dimensional statistical inference. Accordingly, we have chosen to treat our spectral population as a statistical population, with uniform prior probabilities for appropriately selected source and shielding variables. As a result, we can generate representative populations and apply statistical techniques to estimate and extract the information content of the samples drawn from them.

3.1.1 Developing an information-content metric

We have chosen to view these spectral populations in their entirety using what is probably the best-known technique for dimensionality reduction, Principal Component Analysis (PCA) [J1]. The goals of PCA, dimensionality reduction and independence, are achieved by transforming a multivariate data set in such a manner that only a small fraction of new, uncorrelated, dimensions (principal components), are needed to retain nearly all of the variation present in the original data set. In the following section, we will show that, for any particular energy resolution, the number of principal components (dimensions) required to explain a particular desired fraction of the variation in the original data (e.g. 99.9%) provides a measure of the information content available in the original spectral population.[9]

So, what is PCA? Using our geometrical description of gamma-ray spectra being points in a multi-dimensional space, PCA can be qualitatively envisioned as a two-step coordinate

[9] Why use PCA instead of another transformation? PCA's properties of parsimony and independence are superb, and it is theoretically the optimum transform for given data in least-square terms, so it can be applied to a wide range of problems. Although PCA produces the optimum transform and is well suited for this study, it may not be the optimum algorithmic approach for analysis of real-world data. This is because it is very sensitive to deviation from the assumption that the correlation library generated by the analysis accurately describes all real-world measurements. For our simplified problem, this assumption is met as the library produced is defined to cover completely our simplified "universe" of possible measured spectra.

translation: (1) a translation of the coordinate system to center the data at the origin and (2) a rigid rotation of the translated coordinate system to establish the principal components. **Figure 5** illustrates this for trivariate data. In the figure, the data vectors (in our case gamma-ray spectra) are represented as an ellipsoidal point swarm. The first three axes, translated from "channel space" to center the data are illustrated and are denoted by X_1, X_2, and X_3. A rigid rotation of the axes aligns the new coordinate system such that the first principal component Y_1 lies along the major axis of the ellipsoid representing the direction of maximum variance in the vector population. The second principal component Y_1, representing a rotation about Y_1, aligns along the direction of next greatest variance in the population. This continues with each succeeding new principal component accounting for the direction with the maximum remaining variance until all dimensions are exhausted.

As illustrated by our qualitative geometrical example, the new axes are sorted by their fractional contribution from greatest to least variation. Using linear combinations of all of the new dimensions, any of all of the original spectra can be exactly reproduced. Discarding the dimensions that contribute the least amount of information, approximate reconstructed signals can be built from linear combinations of the remaining dimensions (principal components) that contribute the most to the information content. The more principal components included in the reconstruction, the better its approximation of the uncompressed signal. The more principal components that are required to reconstruct a signal to a given accuracy, the more information content is included in the reconstructed signal. *The number of principal components (dimensions) that we find to be required to achieve a desired level of accuracy for any particular energy resolution is a measure of the information content available.*

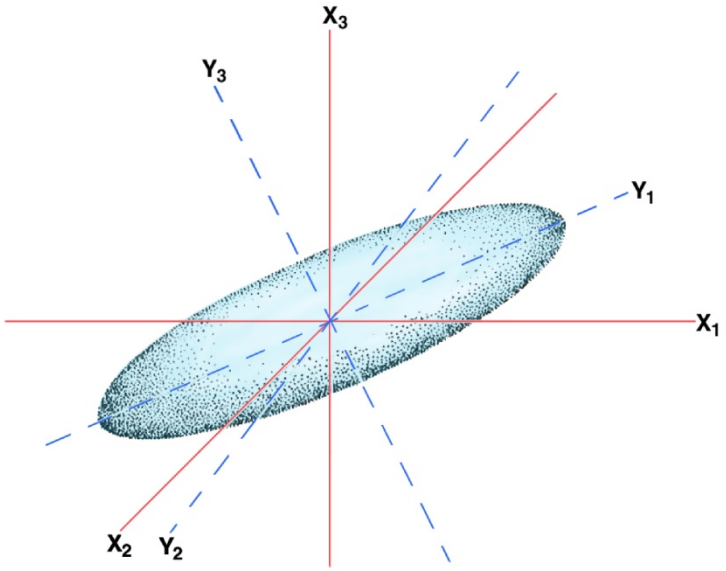

Figure 5. A trivariate vector population is represented as an ellipsoidal point swarm. The first three axes, translated from "channel space," are illustrated and are denoted by X_1, X_2, and X_3. A rigid rotation of the axes aligns the new coordinate system along its principal components, Y_1, Y_2, and Y_3. Figure is adapted from [M3].

The ellipsoidal representation of a data population in Figure 5 is schematic only and not representative of real data. Such a dense and tightly defined cluster would not represent well-

defined, separable signals. Gamma-ray spectra that are of interest in our study, on the other hand, will separate into small near-linear clusters in principal component space for each type of source. Each point in the near-linear cluster will represent differing amounts of shielding. This is illustrated in **Figure 6**.

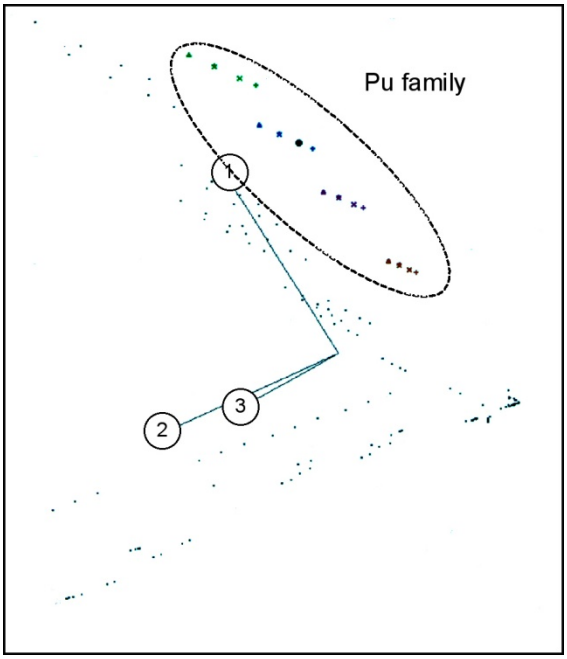

Figure 6. This figure shows the first three principal components from a test library containing 160 computed gamma-ray spectra, representing a variety of gamma-ray sources. We illustrated only the first three principal components because only three components can be represented on the spinning plot capability of the software package used to generate the figure. The rows of dots in the ellipse represent plutonium assemblies of four different ages (elapsed time following chemical purification) and each with four different thicknesses of shielding.

3.1.2 Analytical method used to generate principal components for this study

To perform a PCA analysis of signals, one generates or observes the feature vectors (in our case, gamma-ray spectra) for a population of signals, generates the correlation matrix for the feature space, and computes eigenvectors for that matrix. These eigenvectors are orthogonal basis functions, and any signal in the population can be represented as a linear combination of them. The eigenvectors are then sorted by the magnitude of their corresponding eigenvalues, which is equal to the fraction of the variance between the signals in the population that can be accounted for by each eigenvector. As a result, the eigenvectors are now sorted by their "importance" in representing the signal. We retain those eigenvectors that describe some desired fraction of the variation (the principal components) and discard the rest.

Because the correlation matrix is always symmetric, the generation of the eigenvectors can be accomplished by means of a Singular Value Decomposition (SVD) of the matrix. The sum of the eigenvalues for the correlation matrix is always 1, so the magnitude of each is the fraction of the total variance accounted for by the corresponding eigenvector. We will take the eigenvectors produced from the PCA analysis as the basis functions for all further analyses.

For our scheme, the feature vector is simply the gamma-ray energy spectrum broken into equally spaced energy bins, as is typically observed in any gamma-ray spectrum measurement. As a result, the basis functions can be thought of as "principal spectra," although they are not constrained to be valid spectra themselves. In particular, the functions can have negative magnitudes at some energies, while measured spectra cannot.

The correlation matrix is calculated from the mean and variance for each energy bin from a set of spectra. For a set of N spectra, with amplitude x_{ji} for energy bin j of spectrum i, the mean and variance are calculated by:

$$\boldsymbol{\mu} = \left[\frac{1}{N} \sum_{i=0}^{N} x_{ji} \right]$$

$$\boldsymbol{\sigma}^2 = \left[\frac{1}{N} \sum_{i=0}^{N} x_{ji}^2 \right] - \boldsymbol{\mu} \bullet \boldsymbol{\mu}$$

where " $\bullet$ " is the Hadamard product of the vector of means with itself. The correlation matrix is then given by:

$$R = \left[\frac{1}{N} \sum_{i=1}^{N} \mathbf{x}_i \mathbf{x}_i^{\,T} - \boldsymbol{\mu}\, \boldsymbol{\mu}^T \right] \bullet \left[\boldsymbol{\sigma}^{-1}\, \boldsymbol{\sigma}^{-1^T} \right].$$

To estimate the information content of a set of spectra, we count the number of basis functions, ordered from most to least significant, required to account for some constant fraction of the variance among spectra. In essence, this method estimates the amount of information required to reconstruct a spectrum to some pre-determined accuracy.

We made one change to the standard PCA methodology: because gamma spectra do not have any signal above the highest gamma energy detected, they will have many zero-valued features that do not vary between the spectra in a population. These higher-energy bins can cause numerical instability in the PCA decomposition. To correct for this effect, we add a small constant variance to each feature (energy bin).

3.2 Information content of noise-free generalized spectra

To establish the ability of our procedure to measure the differences in information content between arbitrary spectra of different energy resolutions, we performed the PCA analysis on a set of synthetic spectra. First, we created a set of theoretical gamma sources with evenly-spaced gamma energies from 20 keV to 3 MeV in 0.5 keV steps. These sources were then convolved with theoretical detector energy responses of different resolutions. For each energy resolution, the PCA analysis was performed and the number of principal components required to reproduce the spectra to a given accuracy was determined.

Because of memory limitations, the synthetic spectra were limited to 3000 channels; however, the resulting energy bin size is finer than the best resolution tested, so it should not significantly affect the validity of the results. Examples of the number of principal components required to explain a specified fraction of the variance from 3000-channel spectral data are shown in **Figure 7**. The choice of a benchmark accuracy is essentially arbitrary and made to suit the

analyst's particular need; for this phase, we chose to calculate the number of principal components required to account for 99%, 99.9%, and 99.99% of the total variance.

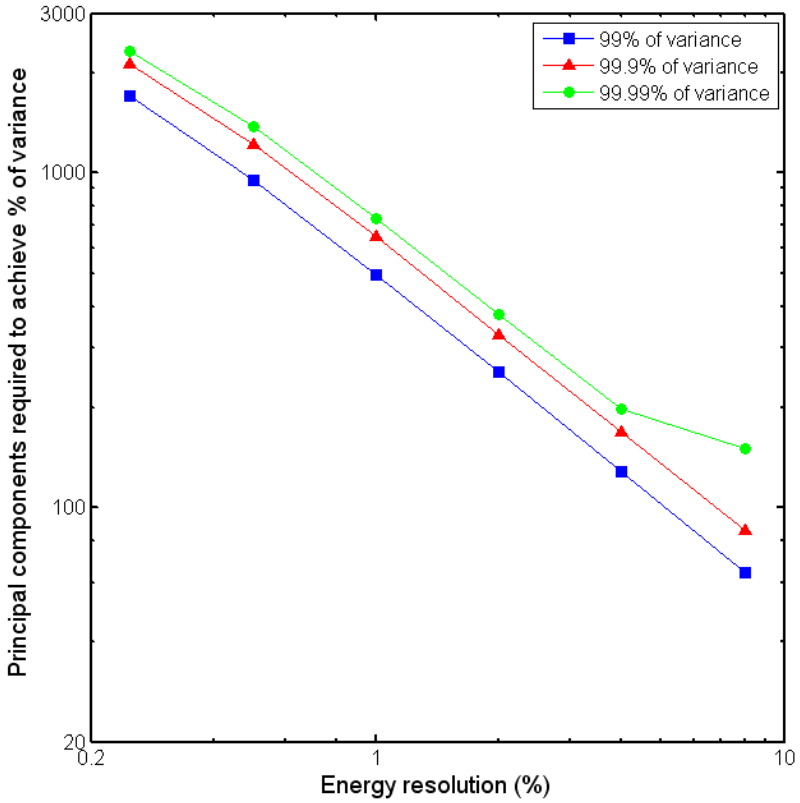

Figure 7. Number of principal components required to explain the specified fraction of the variance between the approximated and exact spectra with evenly-spaced gamma energies. The values plotted for 0.25% resolution are lower limits. At 8% resolution, the bend in the 99.99% curve is due to numerical limitations.

Figure 7 shows that the information content of a spectrum scales nearly linearly (on a log-log plot) with detector energy resolution. The behavior is the same for the three accuracy benchmarks, confirming that the exact choice is not important.[10] From these results, we conclude that our quantitative metric of information content works well and behaves as expected.

3.3 Information content of noise-free spectra from radionuclides

For actual spectra emitted by radionuclides, the gamma-ray energies are much more constrained than in the previous simulation. A real-world radioactive source will emit a set of gamma rays with energies defined by nuclear transitions; the set of all real radioactive sources does not cover the entire set of possible gamma energies.

[10] For a required number of principal components greater than approximately 2000, this method does not produce very meaningful values, because our theoretical spectra only include 3000 energy bins. As a result, it is clear that the information content for the highest resolution is limited by the number of bins in the theoretical spectra. Since each library consisted of 6000 spectra, the theoretical maximum information that could be retrieved is 99.98%; this fact is well represented by the small change in required principal components between 99.9% and 99.99%.

As a result, a more realistic measure of the impact of resolution on the ability to distinguish radioactive sources should use a set of sources with energies corresponding to real-world radionuclides and with various amounts of shielding to simulate real-world detection problems.

First, we selected real-world radionuclides for which to generate simulated spectra. To begin, we included radionuclides with a half-life greater than 10 days. Because this choice does not include medical nuclides that are specifically chosen to have short half-lives, we added commonly used medical radionuclides with gamma energies above 40 keV. We then added specific mixtures of special interest, such as weapons-grade plutonium. Although, in principle, these nuclides are already included as linear combinations, the mixtures were included to ensure that they would be properly characterized. A complete listing of the nuclides used in these simulations is given in **Table 2**.

It should be noted that real-world gamma-ray sources are still more constrained than the set chosen, because certain sets of nuclides always appear together and are unlikely to be separable. Nonetheless, this library of sources provides a reasonable set of constraints.

Because the attenuation of the gamma-ray signal by shielding is a strong function of both the thickness and material type of the shielding, the generation of shielded spectra that span the vast range of real-world possibilities is impractical. We chose to simplify this problem by choosing three representative materials for shielding: Z = 3 (Li) for low-atomic-number shielding, Z = 26 (Fe) for medium-Z shielding, and Z = 82 (Pb) for high-Z shielding.

Table 2. Radionuclides included in the resolution study of noise-free radionuclide spectra. In the upper left-hand corner, RG stands for reactor grade and WG stands for weapons grade.

Pu, RG	^{58}Co	^{91}Nb	^{111}In	^{134}Cs	^{156}Eu	^{190}Ir	^{232}Th	^{240}Pu
Pu, WG	^{59}Fe	^{92}Nb	^{113}Sn	^{136}Cs	^{160}Tb	^{192}Ir	^{232}U	^{241}Am
U, WG	^{60}Co	^{95}Nb	^{114}Sn	^{137}Cs	^{166m}Ho	^{194m}Ir	^{233}U	^{241}Pu
^{7}Be	^{65}Zn	^{95}Zr	^{123}I	^{139}Ce	^{175}Hf	^{201}Tl	^{234}Th	^{242}Pu
^{18}F	^{67}Ga	^{99}Mo	^{123m}Te	^{140}Ba	^{176}Lu	^{202}Tl	^{234}U	^{243}Am
^{22}Na	^{68}Ge	^{99}Rh	^{124}Sb	^{141}Ce	^{177}Lu	^{203}Hg	^{235}U	^{244}Cm
^{22}NaF	^{75}Se	^{99}Tc	^{125}Sb	^{144}Ce	^{177m}Lu	^{204}Tl	^{236}Np	^{249}Cf
^{40}K	^{85}Kr	^{99m}Tc	^{126}Sb	^{147}Nd	^{182}Ta	^{207}Bi	^{236}Pu	^{252}Cf
^{46}Sc	^{85}Sr	^{103}Pd	^{127}Xe	^{152}Eu	^{188}Pt	^{210}Po	^{236}U	
^{51}Cr	^{86}Rb	^{103}Ru	^{131}I	^{153}Gd	^{190}Ir	^{226}Ra	^{237}Np	
^{54}Mn	^{88}Y	^{106}Ru	^{131m}Xe	^{153}Sm	^{192}Ir	^{227}Ac	^{238}Pu	
^{56}Co	^{89}Sr	^{109}Cd	^{133}Ba	^{154}Eu	^{194m}Ir	^{228}Th	^{238}U	
^{57}Co	^{90}Sr	^{110m}Ag	^{133}Xe	^{155}Eu	^{188}Pt	^{231}Pa	^{239}Pu	

The thicknesses of the shielding materials used were selected by a method designed to provide uniform coverage of potential shielding configurations. First, a spectrum with no shielding was produced. Spectra with increased shielding thickness were generated such that the chi-square distance between the spectra generated for successive shielding thicknesses was equal to a fixed value. The size of the chi-square spacing was chosen to be 1 standard deviation for a spectrum containing 10,000 counts in a 1% resolution detector. The number of shielding configurations required for each gamma source varied with the complexity and energy of the source.

These theoretical shielded spectra were convolved with detector response functions in exactly the same manner used for the evenly spaced gamma energies. The number of principal components required to reconstruct the spectra to a given accuracy were determined, as shown in **Figure 8**.

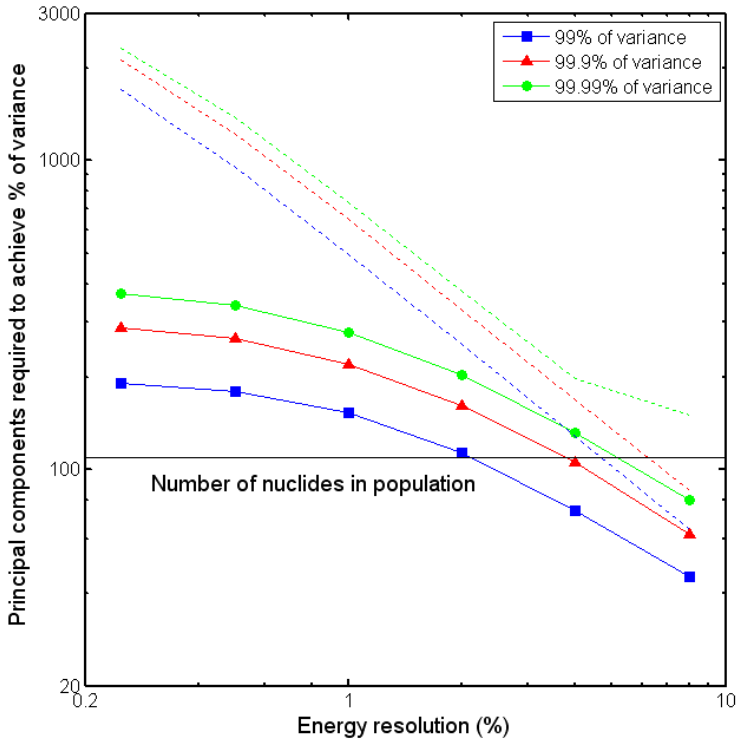

Figure 8. Number of principal components required (out of 3000 possible) to reconstruct, with a given accuracy, noise-free spectra for the radionuclides in Table 2 with various shieldings.

- As expected, the information content of the radionuclide spectra is considerably smaller than for the arbitrary spectra; the natural sources do not span the space of all spectral shapes that the 3000-bin spectra could represent.
- The number of principal components needed could be loosely interpreted as the number of radionuclides that could be uniquely identified for a given resolution. Note that for the worst resolution considered (8%), the number of principal components required to represent all of the information in the set of spectra is far less than the number of nuclides used; this behavior means that for such detectors, some combinations of nuclides are indistinguishable. The resolution is simply not sufficient. At high resolutions, the curves converge to a few hundred principal components since this is all the information content that exists in the spectral data (~100 nuclides and 2 to 4 dominant lines per nuclide).
- These results show that the greatest gains from improved resolution occur for the worst resolutions: halving the resolution from 8% to 4% gives a 70% increase in information content (number of principal components), while halving from 0.5% to 0.25% only gives a 7% increase. While the latter result is (to a small extent) a reflection of the limited number of channels in the theoretical spectrum, the pattern is clear: going to higher and higher resolutions for radionuclide spectra does not provide the gains in information one would expect from a naïve analysis.

3.4 Information content of radionuclide spectra with statistical noise

The previous analyses assumed no statistical noise in the theoretical gamma spectra; the analyzed spectra would be obtained by a detector counting for an effectively infinite time. In reality, very long measurement times are rarely possible, and statistical noise is a significant factor in real-world detection scenarios. We treat this issue of "counting statistics" by examining a range of counts that might be observed in a detector.

To obtain estimates of the effect of statistical noise on the information content of spectra, we assume that the noise for each energy bin is independent and Poisson-distributed, which are both good approximations of the real world. For this case, the statistical noise only affects the diagonal elements of the correlation matrix and can be easily computed from the means of each theoretical spectrum scaled by the total number of counts in the spectrum.

A more exact measurement could be achieved by a Monte Carlo method in which Poisson noise could be added to the theoretical spectra, but such a study would be very expensive computationally and not likely to provide greater insight.

For spectra containing statistical noise, the interpretation of the number of principal components required to model a spectrum to a given accuracy is no longer a straightforward measurement of the spectral information, since the statistical noise also adds (useless) information. As principal components are added, at some point the additional information is only being used to describe statistical noise, not for real spectral information. *This point corresponds to the maximum amount of spectral information that can be extracted from a noisy spectrum*.

We have developed a graphical technique that allows us to estimate the point at which the maximum spectral information is reached. As shown in **Figure 9**, the point at which information from spectral noise begins to dominate appears as the "knee" in the graph of eigenvalue magnitude versus sorted eigenvalue position. Beyond this point, all the eigenvalues have essentially equal magnitude, as expected for noise. As a result, the position of this knee corresponds to the amount of spectral information that can be extracted from the noisy spectrum.

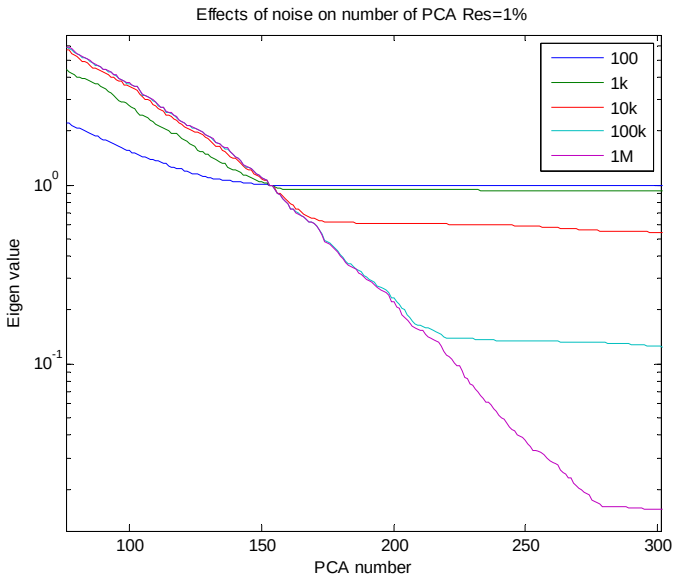

Figure 9. Eigenvalue magnitude versus principal component number for a 1% resolution detector. The values are derived from theoretical spectra with expected Poisson statistical noise from a range of total observed gamma counts. As the number of counts increases, the point beyond which the eigenvalues are equal (the "knee") moves to a higher principal component number. Beyond this point no further information can be extracted.

We performed this same analysis for several detector resolutions (0.25%, 1%, 2%, and 8%) and total spectral counts ranging from 100 to 1,000,000 counts. We extracted the number of principal components at the points where the curves (see **Table 3** and **Figure 10**).

Table 3. Information content of radionuclide spectra with Poisson statistical noise for gamma-ray detectors with a variety of energy resolutions. The value in each cell is the number of principal components where extraction of maximum information content was achieved for spectra with a given number of total counts. These values are the number of principal components at the "knees" in Figure 9 for 1% detectors and from similar plots (not shown) for the other resolutions. The values heavily shaded are the number of principal components required to reproduce 99.9% of the variation in the noise-free spectral population. Values lightly shaded exceed the 99.9% threshold and the additional principal components largely describe only noise.

Total counts	Detector percent energy resolution			
	0.25%	1.00%	2.00%	8.00%
100	140	138	89	43
1,000	158	158	112	54
10,000	199	174	132	62
100,000	252	218	163	72
1,000,000	352	278	208	91

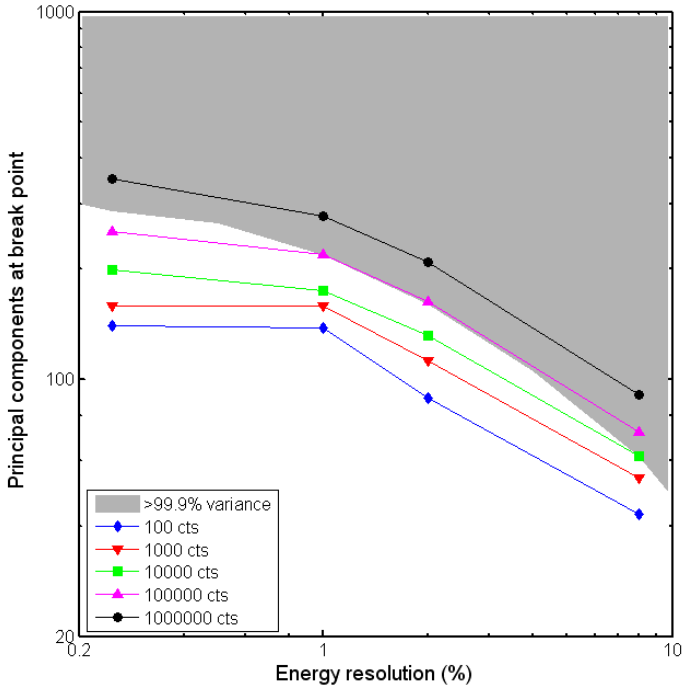

Figure 10. Information content of the same radionuclide spectra as in Figure 8, but with Poisson statistical noise added, for range of energy resolutions. The plotted points are the number of principal components at the "knees" in the curves in Figure 9 for 1% detectors and from similar plots (not shown) for other resolutions.

Several interesting properties can be observed from these results.

- First, we can see that the information content in 100-count spectra can exceed the number of counts in the spectra. This counter-intuitive result occurs because our information is derived from the spectral library as a whole. Thus information, as we have defined it, is a measure of the total information content of all the possible distinguishable spectral shapes that could be obtained from the library and not the information content in any individual spectrum.
- Next, we have shaded the lower portion of Table 3 to indicate the area where full information (in this case, defined as at least 99.9% of variance) has been achieved (see Figure 9). Clearly, the better the energy resolution, the more counts are required to reach the point of complete information. In other words, *the benefit of improved counting statistics is more significant in higher-resolution detectors*. This should not be surprising. A low-resolution detector quickly populates all of the lines available and those low-intensity lines that are masked by poor resolution are never revealed. On the other hand, a high-resolution detector needs more counts to populate those low intensity lines that it can resolve. Nevertheless, even in the suboptimal areas, the high-resolution detector can reveal more information content than low-resolution detectors (8%) or even 2%.
- Finally, the information content between detectors of different resolutions is not as significant for small numbers of counts. For 10,000 total detected gammas, the information from a 0.25% resolution detector only increases by 16% compared to a 1% resolution detector. For 100- and 1000-count spectra, we see that improving the energy resolution from 1% to 0.25% produces no gain in extractable information content at all. This result is counter-intuitive and is a result of our methodology, which only accounts for full-spectrum information. A detection scheme that identifies individual pre-defined full-energy gamma-ray photopeaks could take advantage of the improved energy resolution for small total counts. Such schemes, not addressed by this study, are the preferred analysis method for high-resolution detectors.

3.5 Energy resolution impact on threat/non-threat discrimination

For threat detection scenarios, one is generally less interested in determining the exact isotopic makeup of a source than in distinguishing between threat and non-threat sources.[11] We have, therefore, designed a methodology that allows estimation of the impact of detector resolution for this problem.

To estimate this impact, we calculated bounds on the probability of misclassification of a spectrum for a regression-based identification algorithm as a function of detector resolution. Comments on the preparation of principal components for use in the regression analysis are included in Appendix E. We created a set of spectra corresponding to both threat and non-threat sources for various resolutions, and then estimated the probability of misclassification of the source. To eliminate the effect of counting statistics, we specified a constant number of counts (1000) in the spectrum regardless of resolution.

[11] This application is in contrast to "secondary reachback" screening where one attempts to estimate the isotopic content of a spectrum already determined to be a threat to assess severity. It is in further contrast to a forensic evaluation where one needs to determine isotopic composition to the most accurate extent possible to identify the producer and age of a sample. The resolution requirements are far greater for these latter two applications.

For this phase, we chose specific threat and non-threat scenarios that have proven difficult for existing algorithms to distinguish from a corresponding non-threat or threat [L1]. We approximated a real-world definition of "threat source" by defining a threat as any fissile material or its immediate daughter decay products. We also included ^{241}Am, which builds up in Pu. We identified several nuclides (^{232}Th, ^{40}K, and ^{226}Ra) as natural backgrounds. All other sources were labeled as non-threats.

For each scenario, we generated a theoretical spectrum, and performed three maximum-likelihood fits: one using only threat materials and natural backgrounds, one using only natural backgrounds, and one using only non-threat materials and natural backgrounds. The fitting procedure assumes that the spectrum is a linear combination of the template spectra that were generated for the second phase of this study; each template consists of a nuclide and a shielding material and thickness. A linear combination of templates can be compactly represented as a linear combination of the magnitudes of the principal components for those templates; thus, the fit can be performed in lower-dimensional principal-component space rather than as a fit to the spectra themselves.

For each scenario, we verified that the best fit for the correct class was statistically significantly better than the best fit to background only. We then used the covariance matrix to estimate a multivariate Gaussian uncertainty and used that to estimate the probability of misclassification.

Our results are shown in **Figure 11**. As would be expected, the ability to distinguish threat from non-threat improves as the detector resolution improves. However, the required detector resolution is highly dependent on the details of the scenario.

As can be seen in the figure, for spectra containing 1000 counts, the misclassification rises rapidly for resolutions worse than 1 to 2%, with very small probabilities of misclassification for resolutions better than 1%.

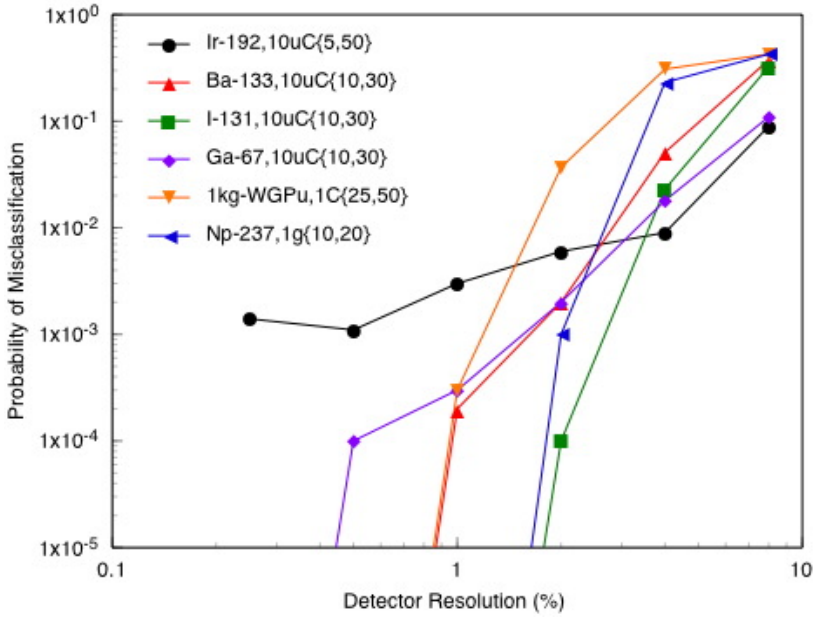

Figure 11. Misclassification probabilities for various scenarios and detector resolutions. The values in braces correspond to the effective *Z* and areal density (in g/cm^2) of the shielding material. All scenarios assume a total of 1000 observed gammas in the detector.

4.0 Conclusions and future work

4.1 Conclusions

This paper presents the first systematic treatment of gamma-ray detector energy resolution, a critical property of gamma-ray detectors used for identification of radionuclides encountered in commerce. We have studied radiation detector resolutions of 0.25%, 0.5%, 1%, 2%, 4%, and 8%, at 662 keV. This wide range of resolutions was investigated to determine what intermediate resolutions might prove useful alternatives to Ge (0.25% or better) and NaI (7–8%). These are the detectors most commonly in use for radiation source identification.

Lanthanum bromide scintillators ($LaBr_3$), with an energy resolution slightly better than 3%, while still small, have recently become commercially available in hand-held radiation identifiers. While still too small for the wide range of applications suitable for Ge and NaI, these detectors can be evaluated with the same systematic approach described in this paper.[12]

We have developed a useful metric to describe the information content of gamma ray spectra as a function of detector resolution. The metric is defined as the number of principal components required to approximate an observed family of spectra to a specified accuracy. It is valid for cases in which the overall shape of a spectrum is being used for radionuclide identification.

We have shown that this metric behaves as expected for synthetic, noise-free spectra, and we have extended it for use in the presence of statistical noise. It allows direct comparison of the ability of detection systems to correctly distinguish between threat and non-threat radionuclide sources. We demonstrated that, at moderate count rates, unambiguous discrimination of potential threat sources from a set of non-threats in the presence of background requires a detector with an energy resolution of approximately 1%. Because our simulations do not account for all of the physical effects that occur in real-world systems, the required resolution may be better than 1%.

This basic study conclusion does not imply that a higher-resolution detector is always preferred over a lower-resolution detector for a given nuclide (or threat) identification application. Other factors must also be considered (e.g., efficiency, cost, size, weight, ruggedness, reliability, comfort, covertness, power consumption, operating temperature and humidity ranges, and user interface). It does, however, establish a quantitative basis for doing comparative evaluations when all other factors are equal. A more complete analysis should be undertaken prior to selecting detectors that includes the factors summarized in the next subsection.

---

[12] Growing large $LaBr_3$ ingots has proven difficult due to the buildup of internal stresses as they cool [D1, M4]. These crystals have a unique drawback; they are radioactive. Natural lanthanum contains 0.09% ^{138}La that decays both by electron capture and β-decay to produce its own complex internal background spectrum that can interfere with weak gamma-ray signals. Nevertheless, a recent study reports: *A series of measurements were performed in late 2006 comparing a 1.5×1.5-in. $LaBr_3$:Ce detector with an Exploranium GR-135 RIID, which contains a 1.5×2.2-in. NaI(Tl) detector. In general, the $LaBr_3$:Ce detector was able to find more peaks and find them faster than the NaI(Tl) detector. To the same level of significance, the $LaBr_3$:Ce detector was usually two to three times faster. The notable exception was for ^{40}K-containing NORM where interfering internal activity due to ^{138}La in the $LaBr_3$:Ce detector exists and NaI(Tl) consistently outperformed $LaBr_3$:Ce.* [M5]

4.2 Future work

In addition to quantifying how frequently errors would occur in field deployments using detectors that cannot unambiguously identify radioactive sources, more insight regarding the importance of detector energy resolution can be gained by addressing other properties of detectors that affect discrimination and identification capabilities.

- For our analyses we compared detectors of equal relative efficiency. It would also be useful to explore the design tradeoffs in material properties and detector volume. For example: one may wish to determine whether a small, high-Z detector or a large, low-Z detector is better. A second tradeoff might compare a small, high-resolution detector to a large, low-resolution detector.
- Thus far, our analysis assumes the detector is modeled perfectly. In practice, one cannot calibrate a detector perfectly. The better the energy resolution, the easier it is to establish the gain calibration. This calibration requirement may further increase the energy resolution requirements for detectors used in the field.
- We employed a number of numerical approximations to avoid having to resort to more computationally intensive Monte Carlo radiation transport calculations. It would be beneficial to run a number of Monte Carlo calculations for a parameter sensitivity study to review those approximations to determine the limitations they impose on interpretation of the results.
- This study concentrated on the intrinsic characteristics of radiation detectors in background-free situations. In real world measurements, background is always present. When radiation from a source incident on the detector is weak, interference from background radiation can be a significant interference to the ability to do source identification. An extension of this work to study the effects of background on detector sensitivity (signal to noise ratio) and its effect of the ability to identify sources would be an important contribution to better understand detector performance under near-real-world conditions.

We do not expect that the suggested additional work would change the fundamental conclusion of the relative superiority of high-resolution detectors for radioactive source identification. We do expect that the current performance gap might increase and drive the need for even higher-resolution detectors, especially with respect to the background issue raised above.

Appendix A: Factors that contribute to the energy resolution of a gamma-ray detector

A-1 Overview

There are a number of sources of fluctuation in the response of a detector that result in imperfect energy resolution. These include statistical noise arising from the discrete number of charge carriers ultimately resulting from gamma-ray energy deposition in the detector, random noise in the detector and associated electronics, drift in the operating characteristics of the detector during the course of measurement, and other sources that will be mentioned in this Appendix.

The overall FWHM of a peak is then a combination of its contributors taken in quadrature

$$(FWHM)^2_{overall} = (FWHM)^2_{statistical} + (FWHM)^2_{noise} + (FWHM)^2_{drift} + ... \quad \text{(A-1)}$$

where the ellipsis indicates other contributors.

Energy resolution also varies as a function of gamma ray energy. This will be discussed last.

A-2 The statistical contribution to energy resolution

Of the contributors to resolution broadening, the statistical contribution represents the irreducible minimum amount of fluctuation in a detector even if the other sources could be reduced to zero. This factor is the statistical noise associated with charge carrier creation. In scintillators the charge carriers are the number of electrons collected from the photocathode of the photomultiplier tube. In a Ge detector, the charge carriers are the electron-hole pairs produced by interaction of a gamma ray in the detector.

Because, for both detector types, the detector voltage pulse has a height that is proportional (nearly for NaI) to the number of charge carriers produced, N, we can express the height, H_0, as

$$H_0 = kN \quad \text{(A-2)}$$

where *k* is a constant of proportionality

If we assume that the formation of charge carriers is a Poisson statistical process and the number of charge carriers generated by full-energy deposition of a gamma ray is N, then $\sqrt{N}$ will be the standard deviation that describes the statistical fluctuation. When N is large, the peak, down to and somewhat below half maximum, will closely approach a Gaussian shape. Since the FWHM of a Gaussian is 2.35 times its standard deviation, σ (see Figure 3), we expect the peak FWHM due to a pure Poisson process to be

$$FWHM = 2.35k\sqrt{N} \quad \text{(A-3)}$$

The fractional resolution due to a purely Poisson process is

$$R_{Poisson} \equiv \frac{FWHM}{H_0} = \frac{2.35k\sqrt{N}}{kN} = \frac{2.35}{\sqrt{N}} \tag{A-4}$$

Measurements of the energy resolution of some types of radiation detectors have shown that the energy resolution can be 3–4 times better than given by Eq. A-4. This indicates that the processes that originate the charge carriers are not statistically independent. This discrepancy can be accounted for by introduction of the *Fano factor*, *F* [F1], a measure of the dispersion of a probability distribution. In the case of a radiation detector, F is defined as

$$F \equiv \frac{\text{observed variance in } N}{\text{Poisson predicted variance in } N} \tag{A-5}$$

Eq. A-4 now becomes

$$R_{Statistical} = 2.35\sqrt{\frac{F}{N}} \tag{A-6}$$

A-2.1 An example comparison of the statistical contribution in NaI and Ge detectors

Knoll provides us with a hypothetical example of the statistical contribution to energy resolution for a gamma ray energy deposition of 500 keV in a NaI detector [K6]. As a result of a scintillation efficiency of 12%, about 25% light loss at the crystal/phototube interface, and a photocathode quantum efficiency of 20%, about 3000 photoelectrons are produced. From Eq. A-6 the statistical contribution to energy resolution, using a Fano factor of 1 for NaI (see Table 1), is

$$\left(R_{Statistical}\right)_{NaI\ @500\ keV} = 2.35\sqrt{\frac{1}{3000}} = 0.043 = 4.3\% \tag{A-7}$$

On the other hand, based on an average of 2.96 eV needed to create one electron-hole pair in a Ge detector, 168,918 pairs of charge carriers are produced in a 500 keV energy deposition. The statistical contribution to energy, using a Fano factor of 0.08 for Ge, is

$$\left(R_{Statistical}\right)_{Ge\ @500\ keV} = 2.35\sqrt{\frac{0.08}{168{,}918}} = 0.0016 = 0.16\% \tag{A-8}$$

A-3 Other contributions to energy resolution in scintillation detectors

For most applications of scintillators the statistical contribution dominates. Electronic noise contributions are usually negligible. Variations in the light collection over the volume of the crystal can be significant. Drifts in the electronics, mostly in the PM tube, can be quite significant especially when temperature varies during measurement.

Another source of peak broadening in most scintillators, including NaI, is their nonlinear response as a function of electron energy. For all but the lowest-energy gamma rays that lead to full energy deposition, multiple interactions are commonplace, typically multiple Compton scatters with a variety of scattered electron energies. As a consequence, even a beam of monoenergetic gamma rays will lead to a wide distribution of electron energies in the crystal. If the response of the crystal is not linear with electron energy, the total light yield will differ from event to event resulting in a broadening of the full-energy peak.

The best performance of a scintillator is given by how well the contributions to resolution loss can be controlled. Our current understanding of these processes places the best possible practical energy resolution of a scintillation detector at about 2%.

A-4 Other contributions to energy resolution in Ge detectors

For Ge detectors, there are three primary contributions to energy resolution, (1) the statistical contribution, (2) noise from all of the electronic components following the detector, and (3) incomplete charge collection that is most notable in detectors of large volume and low electric field.

A-5 Resolution as a function of gamma-ray energy

We note finally that energy resolution is not constant throughout the gamma-ray spectrum but is a function of energy deposition. From Eq. A-3 we see that the statistical contribution to absolute energy resolution increases in proportion with $\sqrt{N}$ and therefore the square root of energy deposition.

Appendix B: Detector efficiency

The interplay of energy resolution and detector efficiency is crucial to detector sensitivity (Appendix C). The detection efficiency of a gamma-ray sensor is a function of its material composition, size, and the gamma ray's energy. To understand the effect of material composition on gamma-ray energy absorption, we need to briefly consider the interaction of gamma rays with matter. Following that will be a qualitative discussion of sensor size and both discussions include the effect of gamma-ray energy.

B-1 Interaction of radiation with matter

For gamma-ray detection, there are three fundamental processes by which gamma rays interact with matter: photoelectric effect, Compton effect, and pair production.

B-1.1 Photoelectric effect

The photoelectric effect occurs when a gamma-ray photon interacts with a single bound atomic electron and the energy of the incident gamma ray is completely transferred to the electron, ejecting it from the atom. The photoelectric effect is especially important for photons with energies below 200 to 300 keV, with all but the lightest elements. The ion produced by the electron ejection will then de-excite by emission of x-rays or Auger electron ejection. These latter radiations locally deposit all of their energy in the sensor,[B-1] resulting in complete gamma-ray energy deposition.

B-1.2 Compton Effect

Gamma-ray photons interacting with electrons can undergo an inelastic scattering process, *Compton scattering*, wherein a fraction of the energy of the incident photon is transferred to an electron and a lower-energy scattered photon is produced. This process gives rise to photons and electrons with a range of energies. Inelastic scattering is the most probable interaction for gamma rays with energies above a few hundred keV for all but the heaviest of elements. In a large detector, a fairly high-energy gamma ray can Compton scatter several times with progressive energy degradation.

B-1.3 Pair Production

Pair production is the name of a process that involves the creation of a positron-negatron pair. It is energetically forbidden for $E_\gamma < 1022$ keV because the creation of two electrons requires at least twice the rest mass equivalent energy of a single electron, 511 keV. The positron will annihilate with a nearby electron and usually produce two 511-keV photons, *annihilation radiation.* For a pair production event to be recorded in the full-energy peak, the two annihilation photons must deposit all of their energy in the sensor.

[B-1] In an extreme counting condition, not encountered in nuclear threat monitoring applications, when an incident gamma ray's energy is low and easily absorbed with a photoelectric interaction near the face of the detector, the photoelectric x-ray can escape from the sensor without energy deposition, resulting in an x-ray "escape peak" appearing below the full-energy peak in the gamma-ray spectrum.

B-1.4 Approximate Z-dependence of the three processes

The approximate Z-dependence of the three gamma-ray interaction processes are summarized in **Table B-1**, as excerpted from [M2].

Table B-1. Processes whereby gamma radiation interacts with matter

Process	Kind of interaction	Significant energy region	Approximate Z-dependence
Photoelectric effect	with bound electrons, causing ejection of electrons	0 to 0.5 MeV (↓ as E_γ ↑)	$Z^{4–5*}$
Compton scattering	with "free electrons"[B-2]	around 1 MeV (↓ as E_γ ↑)	Z
Pair production			
— elastic pair production	with nuclear Coulomb field	> 1 MeV, especially at 5–10 MeV	Z^2
— inelastic pair production	with electron Coulomb field	> 2 MeV (↑ as E_γ ↑)	Z

*The approximate Z-dependence of the photoelectric effect is given in [M1] as Z^5 but is actually a function of Z itself and increases monotonically between 4 and 5 with increasing Z [E2].

B-1.5 Formation of a full-energy peak

All three of these processes can occur following the initial interaction of a single gamma ray. **Figure B-1** schematically illustrates examples of possible single and multiple interactions occurring to three incident gamma rays leading to full energy deposition in a detector.

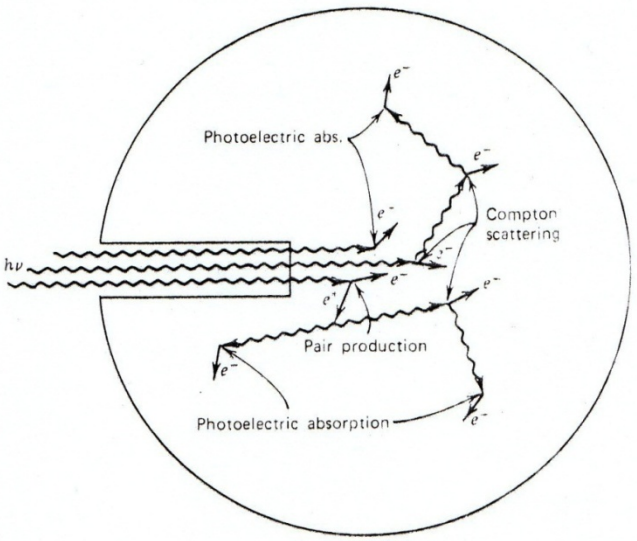

Figure B-1. A schematic illustration of three incident gamma rays that undergo full-energy deposition in a gamma-ray detector. The topmost gamma ray interacts by photoelectric absorption, depositing all of its energy in a single interaction. The middle gamma Compton scatters twice before finally losing its remaining energy in a photoelectric interaction. The bottommost gamma is a high-energy photo that initially interacts by pair production. The resulting positron annihilates creating two 511-keV annihilation photons. The first of these deposits all of its energy by photoelectric absorption and the second initially Compton scatters before a final photoelectric absorption. [K2]

[B-2] Compton scattering occurs at incident gamma-ray energies sufficiently large that, to first order, the electron binding energies can be neglected and the electrons treated as if "free."

We note, as indicated in Figure B-1, that for full energy deposition to occur and a count to be recorded in the full-energy peak, *the final interaction must be photoelectric absorption.* For all but the lowest-energy gamma rays that lead to full energy deposition, multiple interactions are commonplace. They will occur in less than a nanosecond, substantially faster than the response time of all fieldable gamma-ray detectors. Consequently, the detector response appears the same as if the original gamma ray had simply undergone a single photoelectric absorption.[B-3]

B-2 Attenuation and absorption of gamma radiation

The probability of a photon traversing a given thickness of absorber without any kind of interaction is just the product of the probabilities of survival for each particular type of interaction. The probability of traversing a thickness x of an absorber without a Compton collision is just $e^{-\sigma x}$, where σ is the linear attenuation coefficient for the Compton process. Similarly, the probability of no photoelectric interaction is $e^{-\tau x}$ and of no pair production collision is $e^{-\kappa x}$. The magnitude of each of these coefficients is a strong function of gamma-ray energy and the element number Z of the absorbing medium. Therefore a gamma-ray beam of initial intensity I_0, after traversing a thickness x of absorber, will have a residual intensity I of unaffected primary photons equal to

$$I = I_0 e^{-\sigma x} e^{-\tau x} e^{-\kappa x} = I_0 e^{-(\sigma+\tau+\kappa)} = I_0 e^{-\mu x} \tag{B-1}$$

where the quantity

$$\mu = \sigma + \tau + \kappa \tag{B-2}$$

is the *total linear attenuation* coefficient, a function of E_γ and material type. The relative importance of σ, τ, and κ as a function of E_γ is shown in **Figure B-2**.

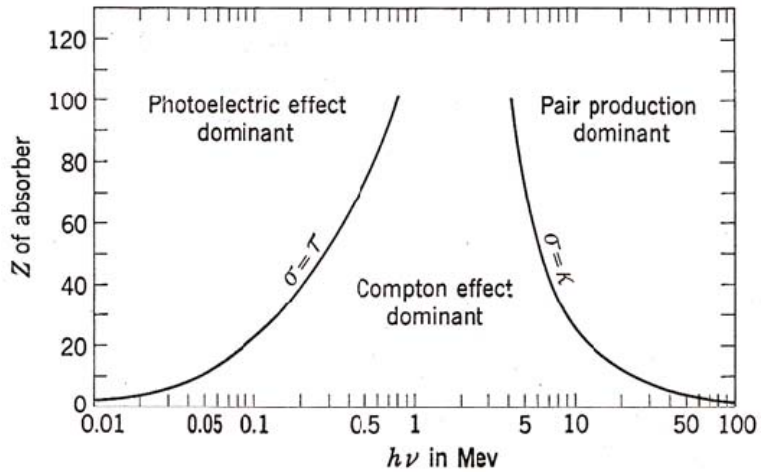

Figure B-2. Relative importance o the three major types of gamma-ray interaction The iso-probability lines show the values of Z and $E\gamma$ $(= h\nu)$ for which the probabilities of two neighboring interaction effects are exactly equal [E1].

[B-3] This statement applies to the monolithic detectors currently applied to threat source detection. It does not apply to segmented volumetric detectors that are not commercial off-the-shelf items.

B-3 Effect of shielding on full-energy peak formation

When doing field measurements, in particular, some intervening material usually shields the source to some extent. This has the effect of attenuating the signal and distorting the shape of the continuum. For full-energy peak modeling this effect is straightforward. Only exponential attenuation occurs as in Eq. B-1. An attenuation term, α, for attenuation by n simple slab attenuators, each with attenuation coefficient μ_j and thickness x_j, is simply the product of the attenuations of each attenuator.

$$\alpha = \prod_{j=1}^{n} e^{-\mu_j x_j} \tag{B-3}$$

The fraction of unattenuated gamma rays, A, is therefore

$$A = 1 - \alpha \tag{B-4}$$

As a result, the total count rate in the full-energy peak, $\dot{P}$, will be diminished in proportion to A and given by

$$\dot{P} = \dot{S} f_\gamma \left(\frac{\Omega}{4\pi} \right) \varepsilon_{ip} A = \dot{S} f_\gamma f_\Omega \varepsilon_{ip} A \tag{B-5}$$

where the rate of gamma ray emissions of energy E_γ is given by the product of the source disintegration rate, $\dot{S}$, and the fraction of nuclear disintegrations, f_γ, that yield that particular gamma ray of interest and can be found in tabulations, e.g. [B1]. The fraction of the gamma rays that will be incident on the detector is proportional to the fraction of the solid angle, $\Omega/4\pi \equiv f_\Omega$, subtended by the detector as viewed from the source. The intrinsic photopeak efficiency, ε_{ip}, is the probability that a gamma ray incident on a detector will record a full energy deposition event in the detector.

B-4 Detector size and efficiency

It is clear that the larger the detector surface area, and therefore f_Ω, that is presented to the source, the more gamma rays that it can intercept. If the detector is also deep enough to provide sufficient volume to absorb all of the incident gamma-ray energy, the full-energy peak efficiency will be nearly proportional to f_Ω. Such is the case with medium- to high-Z sensors for low-energy gamma rays and x-rays. At low gamma-ray energy, the photoelectric coefficient is large and full-energy deposition will occur relatively near the surface of the detector. For applications that only look at these low-energy radiations, thin detectors are used.

B-4.1 Relative sizes of Ge and NaI detectors at the same relative efficiency

Because NaI and Ge are the most often used spectroscopic detectors for threat monitoring, it is useful to compare their detection efficiencies.

So, what are the relative sizes of Ge and NaI detectors at the same relative efficiency? Canberra Industries, a Ge detector vendor, answers this question.

"Coaxial Ge detectors are specified in terms of their relative full-energy peak efficiency compared to that of a 3 in. x 3 in. NaI(Tl) Scintillation detector at a detector to source distance of 25 cm. Detectors of greater than 100% relative efficiency have been fabricated from germanium crystals ranging up to about 75 mm in diameter. About two kg of germanium is required for such a detector." [C2]

Two kg of Ge, with its density of 5.32, occupies a volume of 376 cm^3 while a 3" x 3" NaI detector occupies a volume of 347 cm^3, an 8% volume difference. The fractional linear dimension differences are under 3%. Ge and NaI detectors of 100% relative efficiency are clearly of comparable size.[B-4]

Ge detectors of 100% relative efficiency are currently considered large detectors and we will see that one measure of optimum size for Ge detectors used for threat source identification is somewhat smaller but can reasonable be considered of comparable size to an NaI detector of the same relative efficiency.

B-4.2 The importance of detector volume

It would be desirable to present a simple model to compute a detector's full-energy peak efficiency. However, except for the lowest energy gamma rays that experience only a single photoelectric interaction, no simple model will suffice quantitatively. Examples of the complexity of interactions that typically lead to full energy deposition are shown in Figure B-2. It is possible to accurately model these interactions using the *Boltzmann equation* that, when applied to the transport of gamma rays and neutrons through matter, is called the *radiation transport equation.* Solutions to the Boltzmann equation are arrived at using elaborate computer codes.

To illustrate the importance of detector volume, Stoeffl performed numerous Monte Carlo radiation transport calculations to determine the intrinsic full-energy peak efficiencies of a number of gamma-ray detectors, including NaI and Ge [S2]. The calculations spanned the energy range of 100 keV to 10 MeV in 100 keV intervals and were performed for 13 detector volumes ranging from 1 cm^3 to 8 liters.[B-5]

Figure B-3 illustrates the results of these calculations for Ge detectors. The intrinsic efficiency values on the Y-axis are arbitrary units for comparison only. It can be seen that the efficiency of a 1 cm^3 detector drops by a factor of 100 by 3000 keV, the minimum upper limit of energy typically deemed needed for threat detection. As the volume of the detector increases, the efficiency response curves grow increasingly flatter and the detectors become more useful for the broad energy range needed for threat monitoring. Comparable results are obtained for NaI detectors.

[B-4] A more specific example is given in [T1] in which Canberra Industries supplied the researchers with an actual 100% relative efficiency detector with a volume of 380 cm^3.

[B-5] An 8-liter detector would be truly gigantic, is purely hypothetical, and was computed for illustrative purposes only.

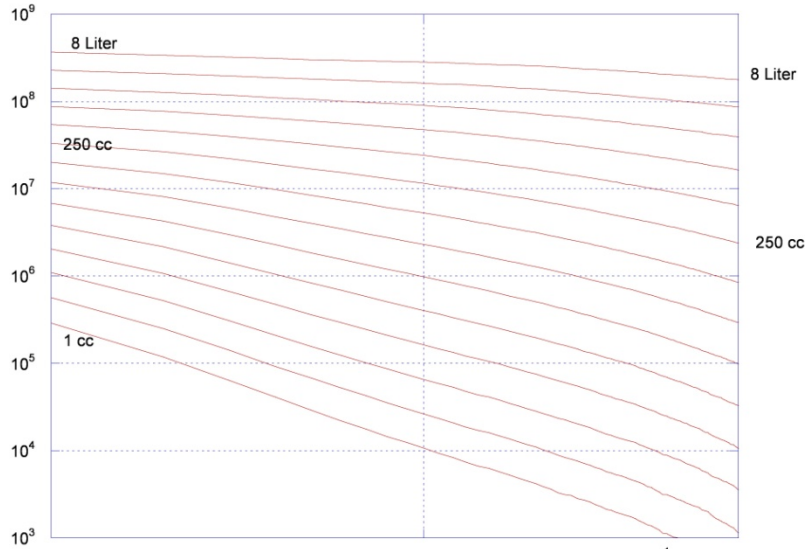

Figure B-3. Ge intrinsic full-energy peak efficiencies over an energy range of 100 keV to 10 MeV in 100 keV intervals and were performed for 13 detector volumes ranging from 1 cm^3 to a hypothetical 8 liters. Efficiencies on the Y-axis are given in arbitrary units.

In **Figure B-4** the results in Figure B-3 have been divided by the detector volume to produce the efficiency per cm^3. This produces two striking results. At 100 keV, a region occupied by many radiopharmaceuticals, the 8-liter detector has the lowest efficiency per cm^3. This is because these low-energy gamma rays are captured at the top of the detector and the bulk of the detector is insensitive. However, this bottom portion of the detector is sensitive to high-energy background gamma rays that downscatter and reduce the detector sensitivity at these low energies (see Appendix C).

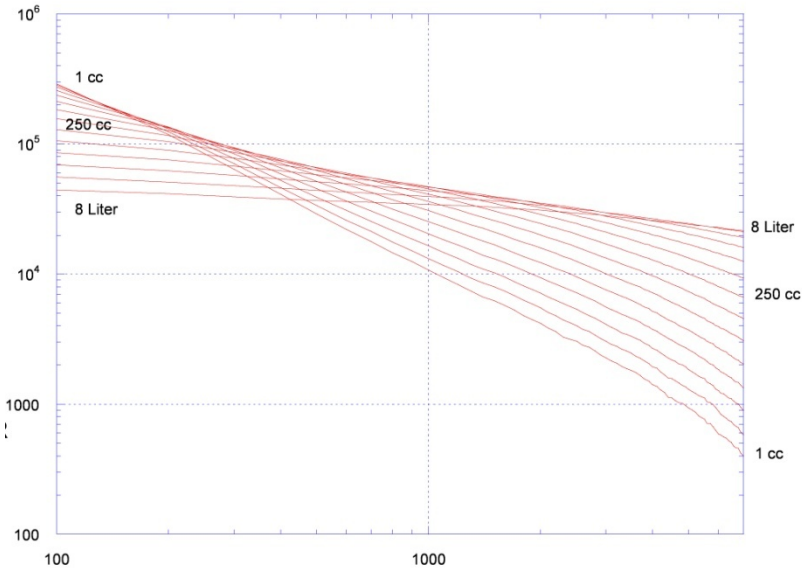

Figure B-4. Ge intrinsic full-energy peak efficiencies per cm^3 over an energy range of 100 keV to 10 MeV in 100 keV intervals and were performed for 13 detector volumes ranging from 1 cm^3 to a hypothetical 8 liters. Efficiencies on the Y-axis are given in arbitrary units.

The second striking result is the crossing of these curves. We can use this crossing to optimize our detector selection. We want good efficiency at low and high energies. The 250-cm^3 detector has relatively good efficiency at 100 keV but drops by less than a factor of 10 at 3000 keV. Such a detector would have about 70% relative efficiency.

Appendix C: Detector sensitivity

Clearly, for a radiation detector, the degree of its response needs to be high enough to detect a useful signal. Moreover, it needs to be high enough to detect this signal within an operationally acceptable period of time in the presence of interferences from natural radioactivity and Compton scattering from higher energy gamma rays originating in the source. The sensitivity is of greatest importance when the interference is comparable to or greater than the source signal intensity. When monitoring for the presence of threat sources, sensitivity is of considerable importance when those sources are shielded and/or weakly radioactive, as in the case of uranium or plutonium.

There are different ways to define detector sensitivity depending on what result is desired. We are not interested in merely detecting the presence of a gamma radiation source but wish to identify the nuclide emitting the radiation. To do this we need to identify a radiation signature from that nuclide in the gamma-ray pulse-height spectrum. The most prominent features of gamma-ray spectra are the full-energy peaks. They are of particular interest for source identification because their energies are unique and well known for benign nuisance sources or possible threat sources that might be observed in commerce. Furthermore, their *position* in the gamma-ray energy spectrum is *invariant* and, unlike the shape of the continuum, is unaffected by shielding or the presence of other peaks (although they can be attenuated to insignificance or masked by other strong gamma rays). For these reasons, one approach to defining spectral sensitivity is to employ a simple traditional model of the full-energy peak signal-to-noise ratio and the time required to detect the peak in the presence of interferences. This model is far from new; it draws on standard references that reach back many years but is nevertheless worthy of review here.

The total count rate in the full-energy peak, $\dot{P}$, is directly proportional to the intrinsic photopeak efficiency, ε_{ip}, and the area of the detector exposed to the source,

$$\dot{P} = \dot{S} f_\gamma \left(\frac{\Omega}{4\pi} \right) \varepsilon_{ip} A = \dot{S} f_\gamma f_\Omega \varepsilon_{ip} A \tag{C-1}$$

where $\dot{S}$ is the source disintegration rate, f_γ is the fraction of nuclear disintegrations that yield the particular gamma ray of interest and can be found in tabulations, e.g. [B1]. Ω is the solid angle subtended by the detector as viewed by the source and determined by the frontal area of the detector. The fractional solid angle subtended by the detector face is f_Ω is equal to $\Omega/4\pi$. Finally, A is a term that accounts for any source attenuation from materials intervening between the source and the detector (see Appendix B).

From Eq. C-1 we see that the total count rate in the peak, $\dot{P}$, is *independent of the energy resolution*. The peak will typically "rest" atop a continuum comprising natural background and Compton downscatter from any higher energy peaks. We assume that we measure the peak over an energy window, R_W, straddling the peak's base on the continuum whose width is proportional to energy resolution (**Figure C-1**).

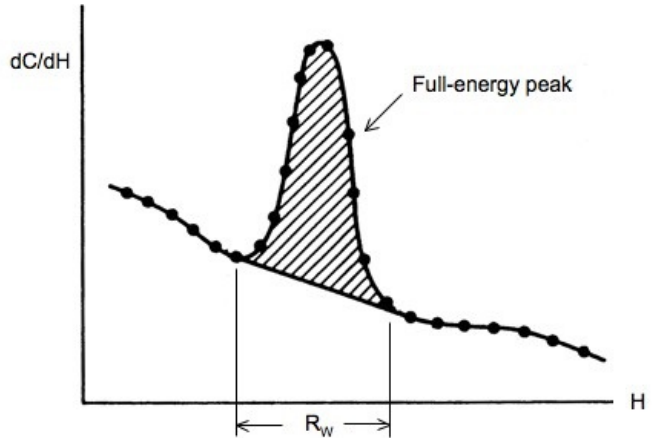

Figure C-1. Schematic illustration of a full-energy peak resting on a continuum from downscatter or background radiation [adapted from K4].

Assuming the continuum count rate at energy E is $\dot{c}(E)$, the average continuum count rate, $\overline{\dot{C}}$, over the energy interval R_W is

$$\overline{\dot{C}} = \frac{\int_{R_W} \dot{c}(E)\,dE}{R_W} \tag{C-2}$$

The noise associated with the peak measurement will be statistical and closely follow a Poisson distribution. The variance of a Poisson variable is equal to the expected mean of the measurement. Its standard deviation, σ_P, is the square root of the variance.

The mean will be the sum of the peak and continuum counts, $\dot{P}t + \overline{\dot{C}}R_W t$. We estimate the peak signal-to-noise ratio, ρ, in units of standard deviation by dividing the number of counts in the peak by the square root of the sum of the number of counts in the peak plus the number of counts in the underlying continuum.

$$\rho = \frac{\dot{P}t}{\sigma_P} = \frac{\dot{P}t}{\sqrt{\left(\dot{P} + \overline{\dot{C}}R_W\right)t}} = \frac{\dot{S}\varepsilon_{ip} f_\gamma f_\Omega A t}{\sqrt{\left(\dot{S}\varepsilon_{ip} f_\gamma f_\Omega A + \overline{\dot{C}}R_W\right)t}} \tag{C-3}$$

This equation reveals that the signal-to-noise ratio is inversely proportional to the square root of the data acquisition time. We can now rearrange Eq. C-3 to develop an expression for the minimum amount of data acquisition time, t_m, needed to achieve a desired threshold signal-to-noise ratio, ρ_T.

$$t_m = \frac{\rho_T^2}{\left(\dot{S}\varepsilon_{ip} f_\gamma f_\Omega A\right)^2}\left(\dot{S}\varepsilon_{ip} f_\gamma f_\Omega A + \overline{\dot{C}}R_W\right) \tag{C-4}$$

This equation reveals some useful insights. We can see that there will always be a fixed minimum time required to detect a peak. In the leading fraction, this time is proportional to the square of the threshold level of confidence, ρ_T, divided by the square of the detector's intrinsic peak detection efficiency. Because $0 < \varepsilon_{ip} \leq 1$, this is a significant disadvantage for small detectors. Small detectors are also at a disadvantage because the leading fraction is inversely proportional to f_Ω^2. For weak peaks where the source emission rate is small relative to the continuum count rate (i.e., $\dot{S}\varepsilon_{ip} f_\gamma f_\Omega A << \dot{C} R_W$), the data acquisition time required to make peak detection *increases nearly in direct proportion to the energy resolution (larger R_W), a significant disadvantage for low-resolution detectors.*

Appendix D: Analysis of gamma-ray spectra for source identification

D-1 Full-energy peak analysis

A Ge detector, with its excellent energy resolution, separates most, but not necessarily all, gamma rays in complex spectra (see, for example, Figure 1, main body of report). This allows peaks to be isolated and for their unique energies to be precisely determined for nuclide identification, a relatively straightforward process. A fieldable instrument that rapidly and automatically performs such an analysis for commonly encountered radiation sources has been commercially available for several years [O1].

D-2 Other gamma-ray spectrum analysis methods

D-2.1 Region-of-interest/peak analysis

It is quite clear from Figure 1 (see main body of report) that the identity of ^{110m}Ag will not be possible from an isolated full-energy peak in the NaI spectrum as none exists. In general, the "smearing" of spectrum structure in NaI gamma-ray spectra increases the difficulty to perform source identification. In a 2004 evaluation of four handheld NaI- and CZT-based radionuclide identifiers [P2], the National Institute of Standards and Technology observed that, "It is particularly difficult to design an identification algorithm that can analyze a broad range of radionuclides." Some of the instruments tested used a fixed spectral region-of-interest method in their algorithm while others attempted to fit peaks and identify them. An important statement in the conclusion of the report was, "47% of either negative or false positive identification should be considered as a significant negative benchmark of these devices."

D-2.2 Full spectrum analysis

A superior method for analyzing NaI spectra is to perform computer simulations of the full pulse-height spectra for all of the sources of interest and place them in a computer library file. An unknown spectrum is analyzed by successively comparing it to a linear combination of measured background radiation and each of the library spectra (and some important combinations of library spectra). This technique, while tedious and complex to develop, works reasonably well but accounting for the effects of source shielding can cause the spectral library to balloon to considerable size (thousands).

D-3 The effect of shielding on source identification

When an absorber is present, the counts in the photopeak, $\dot{P}t$, are attenuated by an amount A but its energy resolution will remain largely unchanged and full-energy peak analysis is possible if isolated, well-defined peaks are available.

For complex NaI spectra with no isolated photopeaks, the analysis is even more difficult than indicated above. Even the difficulty of the full-spectrum analysis method is greatly amplified. Spectra distorted by intervening material present a significant problem with the size of a library because each of the sources of interest would have to be modeled with representative samples and thicknesses of intervening materials. This would likely result in a library of thousands of

spectra. **Figure D-1** shows such a family of curves computed for the commonly encountered radiopharmaceutical ^{67}Ga. Various absorbers were used in the computations, H_2O, Al, Fe, Pb, and some combinations of those. As the absorber attenuation increases, spectral structure degrades beginning with the lowest energy peaks.

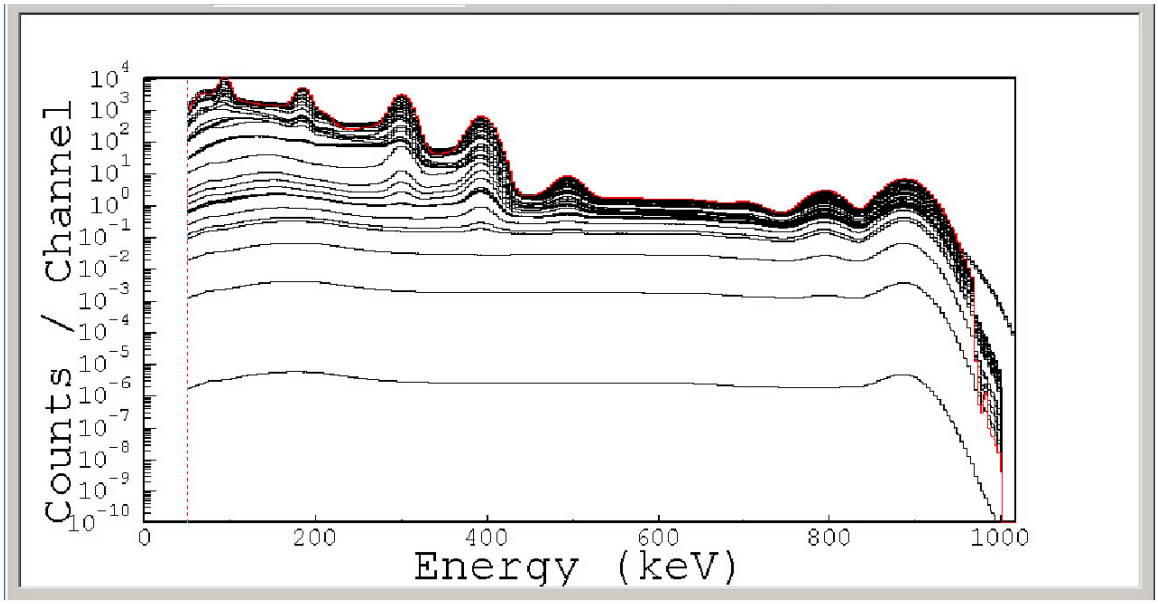

Figure D-1. Computed source library spectral template set for the radiopharmaceutical ^{67}Ga as would be observed with an Exploranium GR135 [S1] NaI detector through various types and thicknesses of shielding. The topmost spectrum in red is for a bare source. The bottommost spectra have been heavily shielded with lead and exhibit an extreme loss in spectral structure [C3].

Appendix E: Methodology for producing principal components

Prior to beginning the analysis for Section 3.4, we tested the Principal Components transform used for comparing spectra. To perform this test, we used the most varying eigenvectors (Principal Components) as a basis of compression. That is, we project each of the samples onto the most varying eigenvectors and thus transform them back to the original space. If the basis we have selected is the proper representation then the differences between the ideal spectra and the transformed spectra should be small.

We found that this was not the case. In fact there were definite statistical differences. This is because the mean of the templates library had a large projection into the eigenvectors which had been discarded as insignificantly varying. This is certainly correct in general that the mean never varies. However, for our problem the mean is just an artifact of the samples we selected for our library and the counts used to normalize the templates. In practice for gamma ray spectra, there is no true expected mean for all spectra. This means our computed mean would result in errors if we used this basis for comparing mixtures in an actual analysis.

To resolve this problem, we examined the procedure used to produce the covariance matrix. In this procedure, we subtract the entire mean from the sample-squared matrix relegating the mean to be a non-varying component. Instead, we could simply reduce the magnitude of the mean to 1% of its original magnitude. This does not change the results of any of the previous analysis and reduces the errors in our compression test to trivial levels. Thus we used this reformulated definition for the analysis in Section 3.4.

[This page intentionally left blank.]

References

A1 G. A. Armantrout, A. E. Bradley, P. L. Phelps, *Sensitivity problems in biological and environmental counting,* IEEE Trans. Nucl. Sci., **NS-19**(1), 107 (1972).

B1 E. Browne and R. B. Firestone, *Table of Radioactive Isotopes,* Wiley, New York (1986). The current version of this compilation is on line at *http://ie.lbl.gov/education/isotopes.htm*

C1 J. A. Cooper, *Factors determining the ultimate detection sensitivity of Ge(Li) gamma-ray spectrometers,* Nucl. Instr. Meth., **82** (1970) 273.

C2 *Gamma and X-ray detection,* Canberra Industries, Meriden CT, USA, http://www.canberra.com/pdf/Literature/Gamma%20Xray%20Det%20SF.pdf

C3 M. Cunningham and T. Gosnell, Lawrence Livermore National Laboratory, private communication (2006).

D1 F. P. Doty, D. McGregor, M. Harrison, K. Findley, R. Polichar, P. Yang, *Basic Materials Studies of Lanthanide Halide Scintillators,* Proceedings of the Materials Research Society, Fall 2007.

E1 R. D. Evans, *The Atomic Nucleus,* p. 712, McGraw-Hill, New York (1955).

E2 Ibid. pp. 698–700.

F1 U. Fano, *Ionization yield of radiations. II. The fluctuations of the number of ions.* Phys. Rev., **72**:26-29 (1947).

H1 R. L. Heath*, Scintillation Spectrometry Gamma-Ray Spectrum Catalogue*, IDO-16880, Vol. 1, p. 6 (1964).

J1 I. T. Jollife, *Principal Component Analysis,* 2nd Ed., Springer, New York (2002).

K1 G. F. Knoll, *Radiation Detection and Measurement,* 3rd Ed.**,** p. 115, Wiley, New York (2000).

K2 Ibid., p. 314.

K3 Ibid., p. 416.

K4 Ibid., p. 341.

K5 Ibid., p. 427.

K6 Ibid., p. 330.

L1 S. E. Labov, L. Pleasance, P. Sokkappa, W. Craig, G. Chapline, M. Frank, J. Gronberg, J. G. Jernigan, S. Johnson, J. Kammeraad, D. Lange, A. Meyer, K. Nelson, B. Pohl, D. Wright, R. Wurtz, *Foundations for Improvement to Passive Detection Systems—Final Repor*t, UCRL-TR-207129 (October 2004).

M1 D. J. Mitchell, H. M. Sanger, and K. W. Marlow, *Gamma-ray response functions for scintillation and semiconductor detectors,* Nucl. Instr. and Meth. A276 (1989) 547.

M2 P. Marmier and E. Sheldon*, Physics of Nuclei and Particles,* Vol. 1, p. 99, Academic Press, New York (1969).

M3 D. F. Morrison, *Multivariate Statistical Methods,* 2nd Ed., p. 275, McGraw-Hill, New York (1976).

M4 P. R. Menge, G. Gautier, A. Iltis, C. Rozsa, V. Solovyev, *Performance of large lanthanum bromide scintillators,* Nucl. Instr. Meth. Phys. Research A, **579** (2007) 6.

M5 B.D. Milbrath, B.J. Choate, J.E. Fast, W.K. Hensley, R.T. Kouzes and J.E. Schweppe, *Comparison of $LaBr_3$:Ce and NAI(Tl) scintillators for radio-isotope identification devices,* Nucl. Instr. Meth. Phys. Research, **572** (2007) 774.

O1 *Detective and Detective-100: HPGe-based Portable Nuclide Identifier,* Ortec, Oak Ridge, TN, *http://www.ortec-online.com/pdf/detective.pdf*.

P1 J. Cl. Phillipot, *Automatic processing of diode spectrometry results,* IEEE Trans. Nucl. Sci., NS-17(3), 446 (1970).

P2 L. Pibida, M. Unterweger, and L. R. Karam, *Evaluation of handheld radiation identifiers,* J. Res. Natl. Inst. Stand. Technol. **109**, 451-456 (2004).

S1 http://www.saic.com/products/security/gr-135

S2 W. Stoeffl, *Monte Carlo calculations of the intrinsic full-energy peak efficiencies of a variety of gamma-ray detectors,* Lawrence Livermore National Laboratory, Personal communication, 2008.

T1 N. Todorivic, D. Mrda, I. Bikit, M. Veskovic, S. Forkapic, j. Slivka, *First tests of the big volume ultra low background gamma spectrometer,* Departman za fiziku, PMF, Novi Sad University, http://www.if.ns.ac.yu/download/39-Todorovic.pdf